Unemployment and the State-Dependent Effects of Monetary Policy

Eva F. Janssens[†] and Sean McCrary[‡]

April, 2024

Most Recent Version

Preliminary draft, please do not circulate without permission!

Abstract

This paper provides empirical evidence that monetary policy has larger and more persistent effects on output, unemployment, and market tightness during times of high unemployment than during low-unemployment episodes. In contrast, we find little evidence for unemployment-dependence in the response of prices and wages. This result implies that the inflation-unemployment trade-off, also known as the Philips Multiplier, is time-varying and procyclical. These results can be rationalized using a tractable New Keynesian model with frictional labor markets, when solved using global projection methods. The main mechanism operates through strong nonlinearities inherent in firm profit and labor demand. The model, estimated using nonlinear full-information Bayesian methods, endogenously generates state-dependent impulse response functions in line with our empirical evidence, and Philips Multipliers that are two times smaller in recessions than during expansions.

Keywords: Numerical methods, discretization filter, labor search

JEL classification codes: C63, C68, E52

* Disclaimer: The views expressed in this paper are solely the responsibility of the authors and should not be interpreted as reflecting the views of the Board of Governors of the Federal Reserve System.

* Acknowledgements: Any errors are our own.

Contact information:
† Eva F. Janssens: Economist at the Division of Research and Statistics, Federal Reserve Board, e-mail: evafjanssens@gmail.com
‡ Sean McCrary: Ohio State University, Department of Economics, 410 Arps Hall, 1945 North High Street, Columbus, OH 43210. E-mail: mccrary.65@osu.edu

1 Introduction

The effects of monetary policy shocks vary over time. In this paper, we study a specific form of state-dependence: the real effects of monetary policy shocks are larger and more persistent when the unemployment rate is high. We show this empirically, and provide a theoretical model to understand the mechanisms behind this phenomenon. In particular, we show that the propagation of monetary policy shocks in a New Keynesian model with labor market frictions is determined by the flow profit of the firm, analogously to how the propagation of technology shocks depends on the *fundamental surplus* in Ljungqvist and Sargent (2017). Since the flow profit is an endogenous state-dependent object, it follows that the real effects of monetary policy also vary with the state of the economy. Solving the model globally and estimating it nonlinearly allows us to preserve and exploit the inherent nonlinearities and state-dependencies in our model, resulting in state-dependent impulse response functions that measure the time-varying effects of monetary policy.

The first contribution of this paper is empirical, providing model-free evidence on how the effects of identified monetary policy shocks depend on the current unemployment rate. We use state-dependent local projections, as in Cloyne, Jordà, and Taylor (2023), combined with regularization techniques. We find that state-dependence matters for the real side of the economy: the industrial production index, the unemployment rate, the job finding rate, market tightness and the number of vacancies. Specifically, we find that during times of high unemployment, the response of these variables to monetary policy shocks is stronger and more persistent, compared to times with low unemployment rates, where the effects are small and short-lived. In contrast, we find little evidence for state-dependence in the responses of wages and prices.

The second contribution of the paper is to propose a structural model that can rationalize the empirical findings. The model combines a standard small-scale New Keynesian (NK) environment (Gali, 2015) with Diamond-Mortensen-Pissarides[1] style labor market frictions, henceforth NKDMP. While this model is small relative to other NKDMP models, for example, Christiano, Eichenbaum, and Trabandt (2016), the focus of our paper is to show these models have strong nonlinearities, revealed by its global model solution, that can speak to the state-dependent effects of monetary policy we see in the data. Key is that our model includes frictional labor markets and bargained wages. In this environment, the movements to marginal cost have very nonlinear effects on labor demand operating through the flow profit of the firm,

[1]Diamond (1982), Mortensen (1982), and Pissarides (1985)

or equivalently, the fundamental surplus of the match (Ljungqvist and Sargent, 2017). Wage inertia leads to pro-cyclical firm profits, so a shock to the marginal cost of the firm is large relative to profits in recessions. This state-dependent ratio of marginal costs to profits leads to state-dependent responses of real variables to monetary policy shocks. Note that apart from these intrinsic nonlinearities, there are no explicit state-dependent primitives in our modeling environment, rather, state-dependence emerges naturally as part of its solution.

It is known that labor search models and NK models are poorly approximated by perturbation solutions.[2] We show that the issues of perturbation methods are aggravated when combining New Keynesian model features with labor market frictions. A global solution method, on the other hand, retains the model's inherent nonlinearities, and, importantly, preserves the state-dependent nature of the policy rules. We find large differences between the linearized and global model solution of the NKDMP model. For example, when evaluated in the same set of parameters, the ergodic sets of the linearized model and global model solution differ substantially. Particularly, in the linearized economy, there is less volatility in real variables such as unemployment and vacancies, than in the global model solution. The solution method also matters for the model dynamics,

Motivated by the large differences between the linearized and global model solution, rather than calibrating the model parameters, we estimate the global model using Bayesian full-information methods.[3] While this is computationally intensive, we use a methodological advancement to make this exercise feasible on a standard desktop computer. We exploit the discrete nature of our global model solution and combine this with the discretization filter of Farmer (2021), showing that once the model is solved globally, the discretization filter gives an evaluation of the likelihood with little additional cost. The global and linear estimation procedures result in parameter estimates that imply considerably different model dynamics.

Our main findings from the estimated NKDMP model solved with global projection methods confirm our empirical analysis, showing that the effects of monetary policy depend on the current unemployment rate in the economy. During times of high unemployment, variables such as output, unemployment, and market tightness respond strongly to monetary policy

[2] As shown by Petrosky-Nadeau and Zhang (2017), models with labor market frictions feature nonlinearities that are poorly approximated by local solution methods like log-linearization. Similarly, Judd, Maliar, and Maliar (2017) show that perturbation-based solutions to New Keynesian models can be prone to large errors.

[3] An important point made by Petrosky-Nadeau and Zhang (2017) that also applies to our model, is that the ergodic (long-run) mean of the model is considerably different from the steady state. Consequently, standard calibration approaches that target the steady state of the model would lead to unreliable inference, motivating our choice for a formal estimation procedure. Similarly, estimating the linearized model and using those parameter estimates for the global model solution can be unreliable in our application.

shocks. On the other hand, during times of low unemployment, the effects of monetary policy are smaller and less persistent. As in the data, there is less evidence for state-dependent effects of monetary policy on inflation. The nonlinearities and frictions in the model generate hump-shaped impulse responses for our main variables of interest, as in our empirical analysis.

An important implication that follows from our results is that the effects of monetary policy vary with the current state of the economy, and in particular, the model implies that the *costs* of monetary policy vary. While we find that the monetary authority is similarly effective controlling inflation during high and low unemployment episodes, however, its effects on labor markets and aggregate output depend strongly on the current state of the labor market. This results in a procyclical Philips Multiplier (i.e., inflation-unemployment trade-off as in Barnichon and Mesters, 2021), where we find the size can be more than two times larger in expansions than during recessions. In normal times, the Philips Multiplier is estimated to be around -0.1, consistent with our reduced-form empirical evidence as well as existing studies, e.g., Barnichon and Mesters (2021) and Hazell, Herreno, Nakamura, and Steinsson (2022). During large recessions featuring high interest rates, such as those during the 70's and 80's, the Philips curve becomes flatter, with Philips Multipliers as low as -0.05.

We use the estimated model to filter the underlying states of the economy, and compute the impulse response functions implied by our global model solution at each point in time. We use this to shed light on the recent so-called "Soft Landing", discussed in, for example, Boocker and Wessel (2023), and show that our model estimates imply that effects of an increase in the interest rate in 2022 was expected to have small effects on unemployment, mostly driven by the fact that the economy was in a good state at the time of the Federal Funds Rate increases. We contrast this to two other episodes in time (1975 and 1980) where the Federal Funds Rate increased, during which, however unemployment and interest rates where high, resulting in sizeable real effects of monetary policy shocks. More generally, by generating time-varying impulse response functions and Philips Multipliers, our model can be used by policy makers to assess the time-varying effects of policy changes on variables of interest.

Outline The rest of this paper is structured as follows. Below, we provide an overview of the related literature. Section 2 presents empirical evidence on how the effect of monetary policy depends on the current unemployment rate. Section 3 presents our New Keynesian model with labor market frictions, and its key mechanism leading to strong state-dependence. Section 4 discusses solution and estimation methods. Section 5 discusses the comparison between the linear and global model, while Section 6 evaluates the state-dependent nature of the model and its implied impulse response functions, the procyclical Philip Multipliers,

and studies impulse response functions and Philips Multipliers during two specific historical events: the zero-lower bound, and the Soft Landing (2022). Section 7 concludes.

Related literature Our empirical results add to an existing literature studying asymmetries and state-dependence of impulse response functions as implied by Structural Vector Autoregressions (SVARs) or local projections, as in Barnichon, Debortoli, and Matthes (2022) and Ben Zeev, Ramey, and Zubairy (2023) for government spending shocks, and Ravn and Sola (2004), Angrist, Jordà, and Kuersteiner (2018), Tenreyro and Thwaites (2016), and Cloyne et al. (2023) for monetary policy. We focus on the role of unemployment as a source of state-dependence. In particular, our results suggest that state-dependence emerging from unemployment is quantitatively more important than state-dependence from economic growth, and its role also seems more important than the role of asymmetries, which were the focus of previous research. Our proposed regularization technique in the empirical section is similar in spirit as Barnichon and Brownlees (2019) and El-Shagi (2019), that is, a Ridge regression that imposes smoothness on the parameters across different horizons.

Our NKDMP model builds on a long tradition of New Keynesian models and models featuring search and matching à la Diamond (1982), Mortensen (1982), and Pissarides (1985), and more recently, a literature merging both, as in Christiano et al. (2016) and Thomas (2011), with other important contributions from Galí, Smets, and Wouters (2012), Blanchard and Galí (2010), Krause and Lubik (2007) and Gertler, Sala, and Trigari (2008). Our main contribution compared to this literature is to show that the NKDMP model has strong state dependence in the real response to a monetary policy surprise, and the estimation of the global model solution.

Our computational framework adapts Judd, Maliar, Maliar, and Valero (2014), where the most important difference is that we discretize the exogenous states using finite-state Markov chain approximation methods, rather than using integration, because this helps us in our estimation procedure. Our computational results contribute to a literature stressing that highly nonlinear models cannot always be solved accurately using perturbation methods, with important contributions from, among others, Petrosky-Nadeau and Zhang (2017), and Judd et al. (2017). The zero-lower-bound episode has renewed interest in global solution methods for New Keynesian models, for example in Fernàndez-Villaverde, Gordon, Guerrùn-Quintana, and Rubio-Ramìrez (2015) and Gust, Herbst, López-Salido, and Smith (2017), but we show that nonlinear dynamics matter also when the zero-lower-bound is not binding. In fact, our model shows the strong evidence for Monetary Policy state-dependence when interest rates are high, rather than low.

In terms of structural estimation, to our knowledge, we are the first to demonstrate and leverage the seamless integration of discrete projection methods and the discretization filter for globally solving and nonlinearly estimating a structural macroeconomic model. Farmer (2021) uses the discretization filter to estimate a second-order perturbation of a model, in which case the discretization filter still requires discretizing the state space, which is computationally intensive. In our approach, we already incur this cost while solving the model, after which the likelihood evaluation is of low additional computational cost. On the other hand, Gust et al. (2017) estimate a globally solved model using the particle filter, in which case both the solution and filtering step are computationally expensive, as large models require many particles, and there are no synergies between solution and estimation. Borağan Aruoba, Cuba-Borda, and Schorfheide (2018), as well as Harding, Lindé, and Trabandt (2022) estimate a linearized version of a DSGE model, and then evaluates the model implications using a globally solved version of the model. While computationally attractive, when the differences between the local perturbation and global solution are too large, as is the case for our model, such an approach may be unreliable.

Finally, our paper relates to a long literature studying the Philips (1958) curve, including its nonlinearities and time variation in its slope, in, e.g., Coibion and Gorodnichenko (2015), Smith, Timmermann, and Wright (2023), and others. Smith et al. (2023) (empirically) as well as Benigno and Eggertsson (2023) (model and empirics) argue the Philips curve is steeper at lower unemployment rates (tighter labor markets), consistent with our empirical and model findings. Benigno and Eggertsson (2023) model this in a New Keynesian framework by assuming a kink in wage setting around a market tightness of one, which mechanically results in a kink in the Philips curve. Instead, we show that state-dependence does not have to be built-in a New Keynesian model, but arises endogenously from its nonlinear model solution. Harding et al. (2022) and Harding, Lindé, and Trabandt (2023) argue non-linearities in the Philips curve are driven by state-dependencies in prices, rather than labor markets, results we view as complementary. Also related is Lahcen, Baughman, Rabinovich, and van Buggenum (2022), who focus on the state-dependent effects of inflation on unemployment, while we focus on the state-dependent effects of unemployment. Our empirical and model-based estimates of the Philips Multiplier are in line with the existing literature, see, for example, Cerrato and Gitti (2022)'s pre-Covid estimates, and Barnichon and Mesters (2021) and Blanchard (2016) post-1990's, which we elaborate on in the results section.

2 Empirical Evidence: State-dependent Regularized Local Projections

This section presents empirical evidence that the effects of monetary policy depends on current labor market conditions, in particular, the current unemployment level of the economy. We show this using state-dependent Local Projections as in Cloyne et al. (2023), in combination with regularization techniques. In addition, we show that, once controlling for state-dependency in the form of unemployment, the role of other state-dependencies, in particular in the form of economic growth or asymmetries, is limited. These empirical results form the motivation for the structural model presented in the next section.

2.1 Methodological Framework

Consider the framework of Local Projections, proposed in Jordà (2005):

$$y_{t+h} = \alpha_h + \beta_h s_t + w_t \gamma_h + \varepsilon_t, \quad \text{for } h = 0, ..., H \text{ and } t = 1, ..., T, \tag{1}$$

where s_t is some exogenous shock, y_{t+h} is the outcome of interest, and w_t is a set of controls, which typically includes lagged values of the shock s_t and the outcome variable y_t. Under the appropriate assumptions, β_h, $h = 0, ..., H$ traces out the *Impulse Response Function* (IRF) of variable y in response to a shock s. Ramey (2016) gives an excellent overview of commonly used shock series s_t for studying the effects of monetary or fiscal policy.

As in Cloyne et al. (2023), we extend this framework to allow for state-dependent impulse responses, based on the so-called Kitagawa-Blinder-Oaxaca (KBO) decomposition. Consider a *state* x_t. The state-dependent local projection then becomes:

$$y_{t+h} = \alpha_h + \beta_h s_t + \beta_h^x s_t (x_t - \bar{x}) + w_t \gamma_h + \varepsilon_t, \quad \text{for } h = 0, ..., H \text{ and } t = 1, ..., T, \tag{2}$$

where the set of controls w_t is now augmented with $(x_t - \bar{x})$, as well as an interaction of all the controls with $(x_t - \bar{x})$. Compared to the local projection in Equation (1), the difference is the KBO term $\beta_h^x s_t (x_t - \bar{x})$, capturing state dependence. The time-varying impulse response function is then traced out by the sum of the direct effect of the shock, $\hat{\beta}_h$, and the state-dependent effect $\hat{\beta}_h^x (x_t - \bar{x})$.

As pointed out in both Cloyne et al. (2023) and Gonçalves, Herrera, Kilian, and Pesavento (2023), it is important that the shock s_t is exogenous to both x_t and y_{t+h}, which, at least contemporaneously we can assume to be the case in our setting. In particular, in our application we use exogenous identified monetary policy shocks for the US, which should be exogenous

with respect to the unemployment rate, as the unemployment rate is part of the Federal Reserve mandate. Future values of the state, however, will be affected by the shock: monetary policy shocks have an effect on the unemployment rate. Note that our set-up is different than, for example, studying asymmetry as a form of state-dependence, which introduces a state that is a direct and non-differentiable function of the shock, which is the focus of Gonçalves et al. (2023). While our set-up is different than Gonçalves et al. (2023), the interpretation of these local projections should still be done carefully, and, following derivations analogous to Gonçalves et al. (2023), we will not be able to recover the conditional average response. Consider a simplified version of Equation (2) where we only consider as control a lagged value of y_t. Then, at time t, i.e. $h = 0$:

$$y_t = \alpha_0 + \beta_0 s_t + \beta_0^x s_t x_t + w_0 y_{t-1} + \varepsilon_t$$

This same equation also holds one horizon further, so we have:

$$\begin{aligned} y_{t+1} &= \alpha_0 + \beta_0 s_{t+1} + \beta_0^x s_{t+1} x_{t+1} + w_0 y_t + \varepsilon_{t+1} \\ y_{t+1} &= \alpha_0 + \beta_0 s_{t+1} + \beta_0^x s_{t+1} x_{t+1} + w_0 \left[\alpha_0 + \beta_0 s_t + \beta_0^x s_t x_t + w_0 y_{t-1} + \varepsilon_t\right] + \varepsilon_{t+1} \end{aligned}$$

To recover the conditional average response, we see that contemporaneous exogeneity is not sufficient, because we also need s_t to be exogenous to x_{t+1}, x_{t+2}, etc., which we know will be violated for our application. However, as pointed out in Gonçalves et al. (2023), we can use these state-dependent local projections to study conditional marginal effects, nearby the steady state $\bar{x}$, for small shocks s_t, even though they may not be valid to recover the conditional average response. This is sufficient for our application, we merely wish to provide empirical motivation on whether variables are more or less responsive to monetary policy shocks depending on the unemployment rate at the time the shock realizes. The impulse response functions we document should therefore merely be interpreted as indicative of the direction of these marginal effects, not as conditional average responses. In particular, the figures we show on the state-dependent local projections are computed under an "all-else-equal" assumption, i.e., that unemployment doesn't move in response to the shock, similar to the figures in, e.g., Cloyne et al. (2023).

Allowing for state-dependence introduces many additional parameters; Equation (2) has more than double the number of parameters than Equation (1). Cloyne et al. (2023) uses cross-country variation to aid inference. The data we use for this section are available on monthly frequency, and we find that this, in combination with regularization techniques, gives us sufficient statistical power to study state dependence.

For our framework, we propose using a simple regularization technique, similar in spirit to El-Shagi (2019) and Barnichon and Brownlees (2019), that is, a Ridge regression that imposes smoothness on the parameters across different horizons. In this Ridge regression framework, we estimate the local projections as one large system, instead of equation-by-equation. Rather than using smoothing splines, as in Barnichon and Brownlees (2019), or penalizing second differences, as in El-Shagi (2019), our method simply includes a small penalty term for large deviations in β_h, as well as β_h^x, from one horizon to the next. That is, we have penalty terms $\lambda_1 \sum_{h=2}^{H-1}(\beta_h - \beta_{h-1})^2$, $\lambda_2 \sum_{h=2}^{H-1}(\beta_h^x - \beta_{h-1}^x)^2$ and $\lambda_3 \sum_{j=1}^{k} \sum_{h=2}^{H-1}(\gamma_h^j - \gamma_{h-1}^j)^2$, that we add to the total sum of squares. Here k is the number of control variables in w. So instead of a Ridge regression that shrinks all parameters to zero, we (mildly) shrink the difference between parameters from one horizon to the next, to avoid big jumps in the impulse response function. We leave the first coefficients, i.e., the initial response β_1, β_1^x and $\{\gamma_1^j\}_{j=1}^k$, unrestricted.

For simplicity, only consider regularization of β_h. Let Y_t be the (column) vector containing y_{t+h} across all horizons $h = 1, ..., H$. X_t is a matrix containing the shock, the element one (for the constant) and the controls w_t, repeated for H rows. Next, write X as the vertically stacked regressors X_t, for $t = 1, ..., T - H$, Y the vertically stacked dependent variables Y_t, and P a matrix with $H - 1$ rows, and $H \times K$ columns, where K is the number of columns of X_t. P has 1's on the diagonal, and -1 on the first upper off-diagonal. Note that in X, the shocks are ordered first. Our Ridge regressor can then be written as the following estimator:

$$\hat{\theta} = (X'X + \lambda P)^{-1} X'Y \tag{3}$$

where the first elements of $\hat{\theta}$ contain the estimates of β_h, $h = 0, 1, ..., H$. We can trivially extend this to allow for regularization of the other parameters.

We follow Barnichon and Brownlees (2019) and use a heuristic asymptotic Newey-West variance estimator:

$$\hat{V}(\hat{\theta}) = T \left[\sum_{t=1}^{T-1} X_t' X_t + \lambda P \right]^{-1} \left[\hat{\Gamma}_0 + \sum_{l=1}^{L} b_l \left(\hat{\Gamma}_l + \hat{\Gamma}_l' \right) \right] \left[\sum_{t=1}^{T-1} X_t' X_t + \lambda P \right]^{-1}$$

where $b_l = 1 - l/(1 + L)$ and $\hat{\Gamma}_l = \sum_{l+1}^{T-1} X_t' \hat{U}_t \hat{U}_{t-l}' X_{t-l}$ with $\hat{U}_t$ the regression residuals. As in Barnichon and Brownlees (2019), we set $L = H$.

Both El-Shagi (2019) and Barnichon and Brownlees (2019) use k-fold cross validation to choose the penalty terms λ. That can be done in our approach too, but in our applications, we opt for

choosing λ conservatively low: enough to smooth out the kinks, but not affecting the overall shape of the impulse response function.

2.2 Empirical evidence on state-dependence

In this subsection, we use the framework presented above to analyze the state-dependent effects of monetary policy on various variables. First, we present our baseline framework, based on the standard Local Projection regressions in Equation (1), and compare them with the regularized LP regressions of Equation (3). For these, we use the monetary policy shock series by Romer and Romer (2004), extended by Wieland and Yang (2020) to 2007. These series capture monetary policy surprises identified using quantitative and narrative records around the FOMC meetings of the Federal Reserve.

The dependent variables of interest are the unemployment rate, the Federal Funds Rate (FFR), inflation based on the Consumer Price Index (CPI), wages, the Industrial Production Index (IPI), the job finding rate, market tightness, and vacancies (HWI: help-wanted-index). More details on the data are available in Appendix A. We follow Ramey (2016), and our control variables include the current values of IPI, CPI, PPI (production price index), and the unemployment rate, as well as four lags of the own variable, IPI, CPI, PPI, the unemployment rate, the federal funds rate, and the shock.

Baseline specification The baseline results are visualized in Figure 1. We scale all IRFs to be a one standard deviation shock of the respective shock series used. As can be seen from Figure 1, we replicate the shape of the IRFs for unemployment, the Federal Funds Rate (FFR), and the Industrial Production Index (IPI) documented in Ramey (2016). As can be seen, our regularization does not affect the shape, but merely smooths out the kinks, as desired. The other variables, not studied in Ramey (2016), move as expected: the job finding rate, market tightness and vacancies (HWI) all go down in response to an unexpected increase in the FFR.

Unemployment-dependent monetary policy Next, we study state-dependence of monetary policy shocks using the regression framework of Equation (2). As our state, that is, x_t in Equation (2), we use (log) unemployment. The assumption for the framework of Equation (2) to be valid is that our monetary policy shocks are exogenous to both the dependent variables as well as to the state, which we believe to be appropriate given the rationale of the monetary policy shock. The resulting state-dependent Local Projections are visualized in Figure 2.[4]

[4]For consistency with the specifications presented in the next subsection, we also include lagged values of Total Factor Productivity (TFP) as control variables, but this does not affect the current results.

Figure 1: Baseline Impulse Response Functions using Romer-Romer shocks

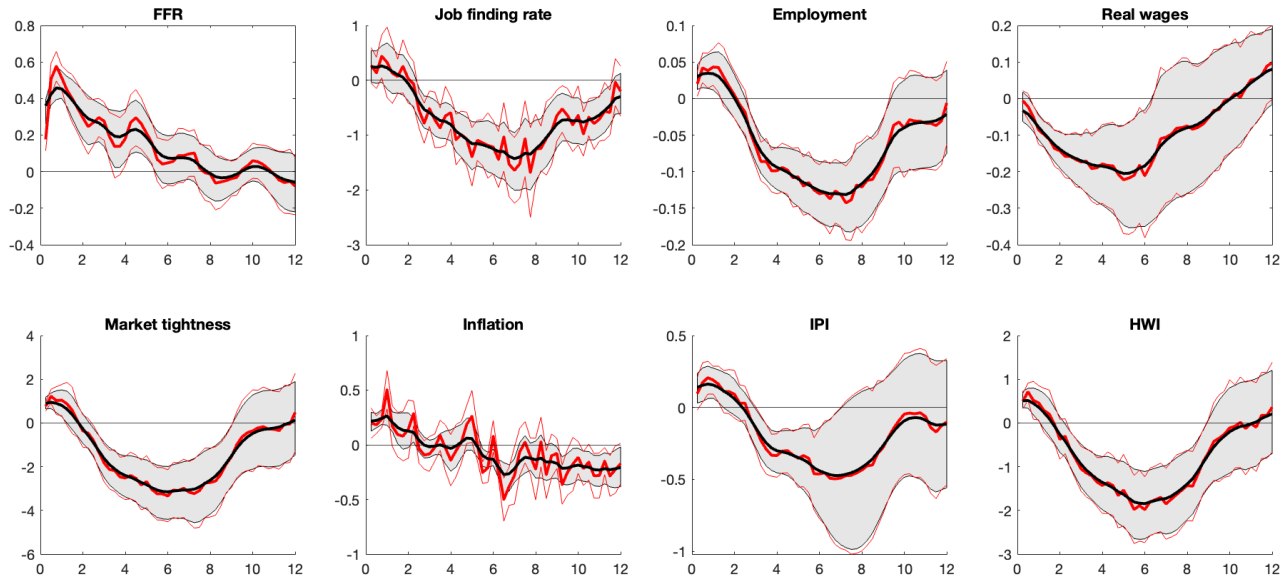

Notes: Thick red line shows the IRF without regularization, thin red lines show the asymptotic confidence interval. Thick black line is the regularized IRF with $\lambda_1 = 100$, there is no state-dependence, so no λ_2, and $\lambda_3 = 0$. The grey bands show the heuristic 90% confidence intervals based on the regularized estimator. Sample 1969-2007, monthly frequency.

For the purpose of this figure, we compute the implied impulse response functions for two different realizations of the state: the 30^{th} percentile of unemployment and the 70^{th} percentile.

As indicative from Figure 2, we find strong evidence for state dependence. In particular, our estimates suggest that for unemployment, the job finding rate, market tightness and the number of vacancies, monetary policy shocks have larger and more persistent effects when the unemployment rate is high. We find little evidence for state-dependence in inflation and wages.

Robustness Our findings are robust to the inclusion of additional lags, shown for six lags in Figure A1 in the Appendix. In addition, we find qualitatively similar results for the monetary policy shock series constructed in Gertler and Karadi (2015) over the period 1990-2012, for which we present results in the Appendix in Figure A2. The shock series of Gertler and Karadi (2015) are noisier, and available over a shorter period, which is why we present the inference based on the Romer and Romer (2004) shocks as our main results. Compared to the Romer and Romer (2004) series, the Gertler and Karadi (2015) series show a somewhat later peak response (around 10 quarters rather than 6-8). State-dependence also seems less strong

Figure 2: State-Dependent Impulse Response Functions using Romer-Romer shocks: low and high unemployment

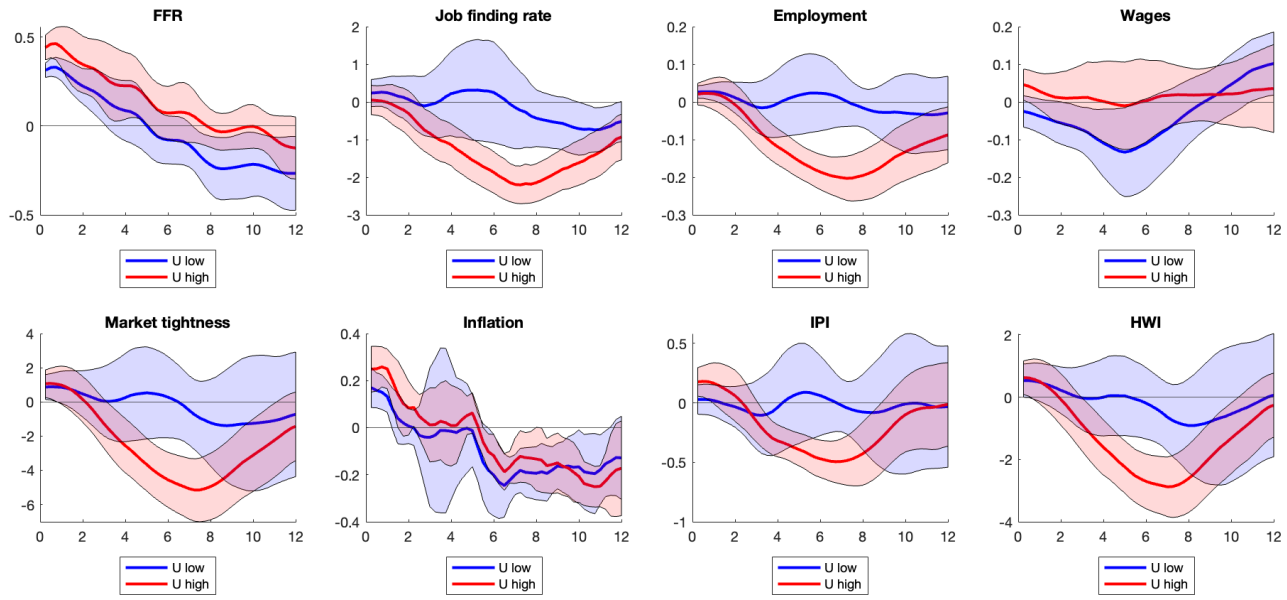

Notes: 90% confidence intervals (asymptotic). Sample 1969-2007, monthly frequency. $\lambda_1 = 200, \lambda_2 = 20$, $\lambda_3 = 0.1$. For the purpose of this figure, the local projections are evaluated in the 30^{th} percentile (low unemployment, blue line) and the 70^{th} percentile of unemployment (high unemployment, red line) over the sample period.

than for the Romer and Romer (2004) shocks. Except for this difference, we find our main conclusions on state-dependence are confirmed by both shock series.

2.3 Other sources of state-dependence

Economic growth The literature has considered other sources of state-dependence, in particular, Tenreyro and Thwaites (2016) analyze whether monetary policy has larger or smaller effects during episodes of high or low economic growth, modeled in a binary fashion. We use our empirical framework to ask whether, once we control for state-dependence in unemployment, we find evidence for state-dependence in economic growth. For economic growth, we use the TFP series of Fernald (2014). This comes down to having two states x_t, one for (log) unemployment, one for TFP growth. The results are visualized in Figure A3 in the Appendix. As follows from Figure A3, controlling for state-dependence in unemployment, we do not find strong evidence for state-dependence in TFP growth. We see this as a refinement of the results in Fernald (2014), decomposing its findings, by saying business cycles consist of both growth (TFP) and employment, and we find it is unemployment that drives most of this state-dependence in monetary policy, with a smaller role for TFP.

Asymmetry Several papers have asked the question whether the effects of fiscal or monetary policy are asymmetric, that is, do unexpected fiscal or monetary policy shocks have different effects when they are negative versus positive? Consider, for example, Barnichon and Matthes (2018), Ben Zeev et al. (2023), Barnichon et al. (2022), Angrist et al. (2018), and others. We ask whether, in addition to state-dependence of unemployment, we can find evidence for asymmetry of monetary policy shocks, by including two (three) x variables: the (log) unemployment rate, an indicator for whether the shock is nonnegative (and an interaction term between the two). The resulting impulse response functions are visualized in Figure A4 and A5 in the Appendix. In short, we find little evidence for asymmetry once we control for state-dependence in unemployment, although state-dependence seems stronger for non-negative monetary policy shocks.

3 A New Keynesian Model with Search Frictions

This section outlines a small-scale New Keynesian DSGE model with search frictions in the labor market a là Diamond-Mortensen-Pissarides. The model economy consists of a perfectly competitive final-goods-producing sector, a continuum of monopolistically competitive intermediate goods producers that set prices subject to an adjustment cost à la Rotemberg (1982) and hire workers by posting vacancies, a continuum of identical households that consume, save in bonds, and supply labor when employed, and a monetary authority that determines interest rates according to an inertial Taylor rule subject to the zero lower bound constraint.

The timing of the model is designed to be able to work with low frequency data (quarterly) in a labor search setting. We assume a model period can be broken down into three sub-periods, (i) job loss and search, (ii) bargaining and production, and (iii) consumption. To deal with the relatively long time periods, we assume workers who lose their job at the beginning of time t are able to find a job within the same period. This allows us to deal with the fact that most unemployment spells are shorter than one quarter without working in a higher frequency setting.[5]. The timeline is visualized in Figure 3.

Details on the solution method and estimation are provided in the next section.

[5]According to the estimate of Ahn and Hamilton (2022), two-thirds of workers exit unemployment within the first quarter of an unemployment spell.

Figure 3: Model Timing

Notes: Z_t is total factor productivity (stochastic), δ is the job separation rate, x_{jt} is the vacancy creation, after which hiring takes place. w_t is the bargained wage, Y_t is the production with the new workers and productivity Z_t. Interest rates are set at R_t by the central bank, and households consume C_t. Vacancies are destroyed at rate ξ, and we move to next period.

3.1 Households

The economy is populated by a continuum of identical households $i \in [0, 1]$ who derive utility from consumption, and supply one unit of labor inelastically to the labor market. The preferences of the representative household are an equally weighted average of its members.

The welfare of household i is given by

$$\mathbb{E}_0 \left[\sum_{t=0}^{\infty} \beta^t D_t \frac{(C_{it} - bC_{t-1})^{1-\tau} - 1}{1-\tau} \right], \tag{4}$$

where b is a measure of external habits, β is the discount factor, D_t is a shock to intertemporal preferences, and $1/\tau$ is the intertemporal elasticity of substitution.

Members of the household perfectly insure each other against variations in income due to unemployment, which implies consumption is identical for all members. This leads to the representative household budget constraint

$$P_t C_t + B_t = W_t N_t + R_{t-1} B_{t-1} + T_t, \tag{5}$$

and the law of motion for employment

$$N_t = (1 - \delta(1 - f_t))N_{t-1} + f_t(1 - N_{t-1}). \tag{6}$$

Here, N_t is the mass of household members who are employed at the production stage, P_t is the price of the final good, B_{t+1} denotes one-period risk-free bonds with gross return R_t, and T_t denotes all remaining income, i.e. firm dividends net of lump sum taxes. The law of motion for employment depends on the exogenous separation rate δ and the endogenous job-finding

rate f_t. The first-order conditions with respect to bonds and consumption imply

$$\lambda_t = D_t \left(C_t - bC_{t-1}\right)^{-\tau}, \tag{7}$$

$$1 = \beta E_t \left[R_t \frac{\lambda_{t+1}}{\lambda_t} \frac{P_t}{P_{t+1}} \right], \tag{8}$$

where λ_t is the marginal utility of consumption. We define the stochastic discount factor used by firms as

$$Q_{t,t+1} = \beta \frac{\lambda_{t+1}}{\lambda_t}. \tag{9}$$

3.2 Firms

Here we outline the production structure of the economy which includes monopolistic producers and labor market frictions.

3.2.1 Final Goods Producers

The finals good producer aggregates intermediate goods $j \in [0, 1]$, using the technology:

$$Y_t = \left(\int_0^1 y_{jt}^{1-\gamma} dj \right)^{\frac{1}{1-\gamma}}. \tag{10}$$

The representative firm maximizes profits

$$P_t Y_t - \int_0^1 p_{jt} y_{jt} dj, \tag{11}$$

taking input prices p_{jt} and output prices P_t as given. Profit maximization implies that the demand for input j is given by:

$$y_{jt} = \left(\frac{p_{jt}}{P_t} \right)^{-\frac{1}{\gamma}} Y_t. \tag{12}$$

We define inflation as $\Pi_t = P_t / P_{t-1}$.

3.2.2 Intermediate Goods Producers

There is a continuum $j \in [0, 1]$ of identical monopolistic intermediate goods producers, with production function

$$y_{jt} = Z_t n_{jt} \tag{13}$$

These firms are monopolists in the product market and competitive in factor markets. Here, Z_t is a neutral technology shock, and N_{jt} is the quantity of labor. Price adjustments are subject to a Rotemberg (1982) adjustment cost given by

$$\frac{\phi}{2}\left(\frac{P_{jt}}{P_{jt-1}} - \Pi^*\right)^2 Y_t,$$

where Π^* is long-run, i.e. target, inflation.[6]

Firms hire labor in a frictional labor market using long-lived job openings. The stock of open jobs is v_{jt}, and newly opened jobs are x_{jt}. Existing openings incur a flow cost κ and are destroyed at rate ξ, while new openings have cost $c(x_{jt})$.

The firm's law of motion for employment and vacancies are given by

$$n_{jt} = (1-\delta)n_{jt-1} + q_t(v_{jt} + x_{jt}), \tag{14}$$

$$v_{jt+1} = (1-\xi)(1-q_t)(v_{jt} + x_{jt}). \tag{15}$$

The firm's problem is to choose employment, vacancies, and prices to maximize:

$$\Pi_{j0} = \mathbb{E}_0 \sum_{t=0}^{\infty} Q_{0,t}\left\{\frac{p_{jt}}{P_t}y_{jt} - w_t n_{jt} - \kappa v_{jt} - c(x_{jt}) - \frac{\phi}{2}\left(\frac{p_{jt}}{p_{jt-1}} - \pi\right)^2 Y_t\right\}. \tag{16}$$

subject to its laws of motion for employment and vacancies, as well as the demand curve (12) for its product. Deriving the first-order conditions with respect to employment n_{jt}, vacancies x_{jt}, and prices p_{jt}, and focusing on a symmetric equilibrium $n_{jt} = n_t$, $p_{jt} = p_t$, and $x_{jt} = x_t$ gives the following equations. The value of the marginal worker is given by

$$\mu_t = (1-\omega_t)Z_t - w_t + (1-\delta)\mathbb{E}_t\left[Q_{t,t+1}\mu_{t+1}\right], \tag{17}$$

where μ_t is the multiplier on the law of motion for employment and ω_t is the multiplier on the output constraint (12). This equation states the marginal job μ_t is the present discounted value of the marginal product of labor $(1-\omega_t)Z_t$ net of the wage w_t, i.e., the flow profit of the

[6]Our motivation for working with the Rotemberg approach to sticky prices instead of the more common approach of Calvo (1983) is to keep the state space manageable. In a global solution, Calvo pricing requires keeping track of price dispersion as an additional state variable, which increases the computational burden of the global model solution.

firm. All else equal, when the firms hire additional workers it must lowers prices to stay on its demand curve, which is reflected in ω_t.

The pricing equation for inflation dynamics is given by

$$\frac{\omega_t}{\gamma} - 1 = -\phi(\pi_t - \pi)\pi_t + \phi\mathbb{E}_t\left[Q_{t,t+1}(\pi_{t+1} - \pi)\pi_{t+1}\frac{Y_{t+1}}{Y_t}\right]. \tag{18}$$

This is a standard pricing equation where the marginal cost is in terms of ω_t. The job-creation condition is given by

$$c'(x_t) = q_t\mu_t + (1 - q_t)(1 - \xi)\mathbb{E}_t\left[Q_{t,t+1}\left\{c'(x_{t+1}) - \kappa\right\}\right], \tag{19}$$

which states the marginal cost of vacancies today reflect the expected value of a match $q_t\mu_t$ plus the saving in terms of marginal costs next period of having a stock vacancy versus posting a new vacancy $c'(x_{t+1}) - \kappa$ in the case the job is not filled. For the remainder, we use the functional form $c(x_t) = \frac{\psi_x}{2}(x_t)^2 + \kappa x_t$ for vacancy costs, so the job creation condition becomes

$$x_t = \frac{q_t\mu_t - \kappa}{\psi_x} + (1 - q_t)(1 - \xi)\mathbb{E}_t\left[Q_{t,t+1}x_{t+1}\right]. \tag{20}$$

3.3 Wage Bargaining

The surplus to the household is the difference between the flow value of employment V_t^e and unemployment U_t, given by:

$$\begin{aligned} U_t &= \nu + \mathbb{E}_t\left[Q_{t,t+1}\left\{f_{t+1}V_{t+1}^e + (1 - f_{t+1})U_{t+1}\right\}\right] \\ V_t^e &= w_t + \mathbb{E}_t\left[Q_{t,t+1}\left\{(1 - \delta(1 - f_{t+1}))V_{t+1}^e + \delta(1 - f_{t+1})U_{t+1}\right\}\right], \end{aligned}$$

where $f_t = \theta_t q_t$ is the job-finding probability. Due to the assumption workers can separate and search within a model period, the effective separation rate is $\delta(1 - f_{t+1})$, i.e., the probability of losing a job and not finding a new job. We define the surplus of a job to the marginal worker as $S_t^h = V_t^e - U_t$, which implies

$$S_t^h = w_t - \nu + (1 - \delta)\mathbb{E}_t\left[Q_{t,t+1}(1 - f_{t+1})S_{t+1}^h\right]. \tag{21}$$

The wage is determined by the Nash sharing rule

$$\eta\mu_t = (1 - \eta)S_t^h, \tag{22}$$

which is the outcome of a bilateral bargain between the representative family and the firm over the value of the marginal job. Here μ_t is the asset value of a job, V_t^e is the present value of employment, and U_t is the present value of unemployment. This leads to an expression that implicitly defines the wage in terms of the present value of a job

$$\mu_t = \frac{1-\eta}{\eta}(w_t - \nu) + (1-\delta)\mathbb{E}_t\left[Q_{t,t+1}(1-\theta_{t+1}q_{t+1})\mu_{t+1}\right], \tag{23}$$

where ν is the flow value of non-employment. Rearranging equations (17) and (23) gives an expression for the wage

$$w_t = \eta(1-\omega_t)Z_t + (1-\eta)\nu + \eta(1-\delta)\mathbb{E}_t\left[Q_{t,t+1}f_{t+1}\mu_{t+1}\right] \tag{24}$$

3.4 Monetary Authority

Monetary policy is determined by a Taylor Rule for the nominal interest rate subject to a ZLB constraint:

$$R_{t+1} = \max\left\{1, \tilde{R}_{t+1}e^{\epsilon_{R,t}}\right\}, \tag{25}$$

where $\tilde{R}_t$ is the systematic component of monetary policy which reacts to the state of the economy, and $\epsilon_{R,t}$ is the shock. We consider the following Taylor rule:

$$\tilde{R}_{t+1} = \left[R_*\left(\frac{\Pi_t}{\Pi^*}\right)^{\psi_1}\left(\frac{Y_t}{Y^*}\right)^{\psi_2}\right]^{1-\rho_R} R_t^{\rho_R} \tag{26}$$

stating the central bank reacts to deviations in inflation and output from their targeted values Π_* and Y^*. In the linear model, we ignore Equation (24), and look at $R_{t+1} = \tilde{R}_{t+1}e^{\epsilon_{R,t}}$ instead.

3.5 Equilibrium Conditions

We assume market clearing in final goods:

$$C_t = Y_t \tag{27}$$

This assumes that vacancy costs and adjustment costs are distributed to the household. This limits the number of state variables we need to consider when solving the model.

Exogenous states evolve according to

$$\ln D_t = \rho_d \ln D_{t-1} + \sigma_d \epsilon_t^d.$$
$$\ln Z_t = \rho_z \ln Z_{t-1} + \sigma_z \epsilon_t^z.$$

Together with Equations (17), (18), (20), (23), (21), the Euler equation of the household, and the law of motions for employment, vacancies and interest rates, these pin down the equilibrium.

3.6 Illustrating the mechanism

To illustrate the mechanism that generates state-dependence in the propagation of monetary policy shocks, this section examines a log-linearized full model of the main text, as well as a smaller version of the model. The log-linearized equations provide intuition as to what matters for propagation in both models.

In the smaller model, we exclude the following model elements: (i) discount factor shocks, (ii) long-lived vacancies (i.e., we only consider a flow, not a stock), (iii) quadratic vacancy cost, and (iv) external habits in the utility function of the households. These four model elements are what generates the persistence and hump-shape in the impulse responses in our model, allowing us to match the empirical evidence of the previous section. However, as we show, these model elements are not necessary for state-dependence in the response to monetary policy shocks.

Appendix Section D presents the log-linearized first-order conditions of both the smaller and full model. Consider the log-linearized job creation condition of the small model, given by

$$\hat{q}_t = \frac{\gamma(1-\beta(1-\delta))}{1-\gamma-w}\hat{\omega}_t - \frac{(1-\gamma)(1-\beta(1-\delta))}{1-\gamma-w}\hat{z}_t + \frac{w(1-\beta(1-\delta))}{1-\gamma-w}\hat{w}_t + (1-\delta)\beta E_t[\hat{q}_{t+1} + \hat{r}_t - \hat{\pi}_{t+1}] \tag{28}$$

where q_t is the vacancy-filling rate. Here the $\hat{x}_t$ notation is used to denote log-deviations of the steady state, where the steady state is denoted by omitting the subscript t.

As can be seen from the log-linearized job creation condition, the sensitivity of q_t to ω_t, w_t and z_t scales inversely with $1-\gamma-w$, the steady state flow profit of the firm, closely related to the *fundamental surplus* in Ljungqvist and Sargent (2017). If the flow profit is small, the propagation of shocks to q_t will be large, and vice versa. Since q_t is the vacancy-filling rate, the same mechanism will determine the propagation of shocks to market tightness and,

consequently, employment and output. In steady state, the flow profit of the firm is given by

$$1 - \gamma - w = (1 - \eta)(1 - \gamma - \nu) - \eta(1 - \delta)\kappa\beta\theta. \tag{29}$$

When this term is small, because the wage w is close to $1 - \gamma$, there is additional sensitivity of labor demand to shocks. All else equal, a higher outside option ν reduces the firm's flow profit by increasing the steady state wage.

The same intution holds for the full log-linearized model, but now the job creation condition is in terms of μ_t, the marginal value of a job to the firm, which determines vacancy creation. The log-linearized job-creation condition is now given by:

$$\hat{\mu}_t = \frac{1 - (1 - \delta)\beta}{1 - \gamma - w} \left[(1 - \gamma)\hat{z}_t - \gamma\hat{\omega}_t - w\hat{w}_t\right] + (1 - \delta)\beta E_t \left[\hat{\pi}_{t+1} - \hat{r}_t + \hat{\mu}_{t+1}\right] \tag{30}$$

Analogously to the smaller model, the sensitivity of μ_t to ω_t, w_t and z_t scales inversely with $1 - \gamma - w$, the flow profit of the firm.

In a log-linearization, we perturb around the steady state, where the surplus is constant. In a global model solution, the surplus of the firm is a time-varying equilibrium object that depends on the state of the economy. A global model solution will therefore endogenously generate state-dependent propagation of monetary policy shocks. To illustrate this mechanism in a log-linear model, we compute the log-linearized solution in two different sets of parameters, one that implies a large surplus (low value of $\nu = 0.60$), and one that implies a small surplus (high value of $\nu = 0.75$). In each case, we recalibrate the matching efficiency χ to target a steady state unemployment rate of 5.76%. This is shown in Figure 4.

As can be seen, in the small surplus economy, the real effects of monetary policy are larger. In addition to showing how state-dependence follows from the size of the surplus, the figure compares the impulse responses from the small and full model, and shows that state-dependence in the size of the response is already present in the smaller model, and does not depend on the introduction of additional frictions in the full model. The full model however introduces persistence and humps in the impulse responses in line with the empirical results of the previous section.

While the real effects of monetary policy depend on the size of the surplus, the figure shows the effects on inflation in both the small and large surplus economy are comparable after the initial impulse. Thus, the log-linearized equations also help us understand why the model generates less state-dependence in prices.

Figure 4: State-dependence in the linearized model: comparing two parameterizations (low and high ν) and two models: simple - bottom row, and full - top row

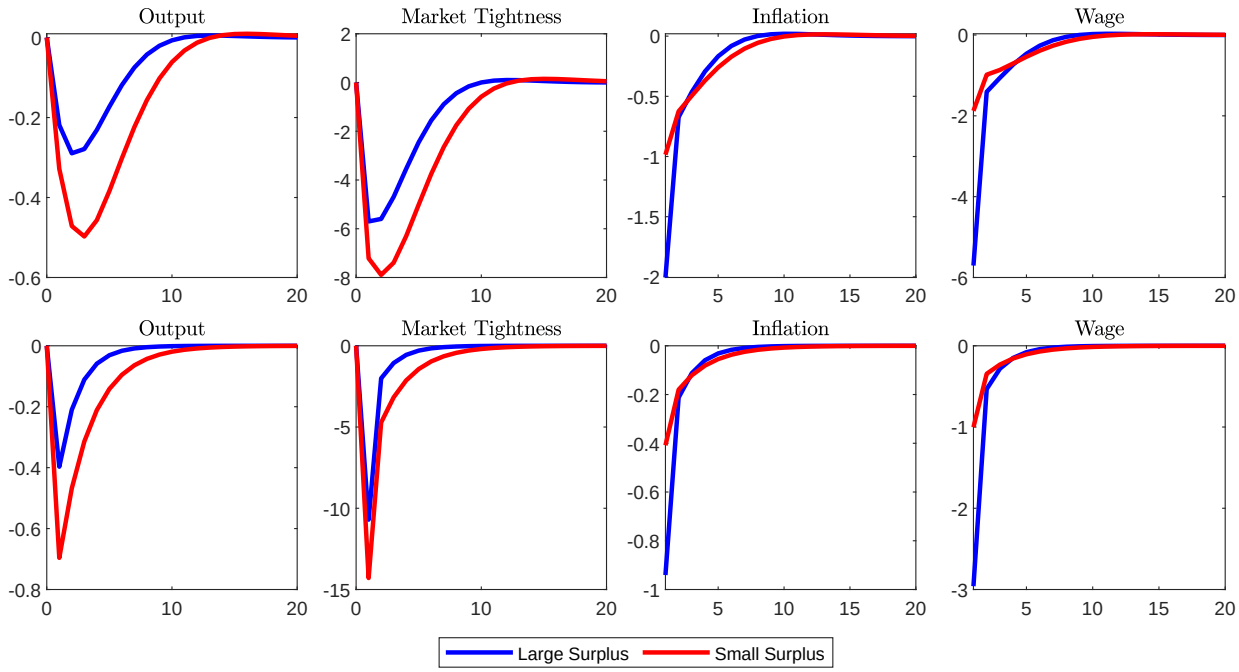

Equation (30) gives the New Keynesian Philips curve of the model, based on the log-linearized pricing equation. As we can see, the sensitivity of inflation depends on the marginal costs ω_t, and scales with ϕ, which is assumed constant. Any state-dependence in inflation would come indirectly from state-dependence in the response of marginal cost, but there is no additional state-dependent propagation in the log-linearized Philips curve. This is consistent with our empirical findings, showing that there is little evidence for unemployment-dependence in the inflation response to a monetary policy shock.

$$\hat{\pi}_t = \beta E_t \left[\hat{\pi}_{t+1}\right] - \frac{1}{\phi}\hat{\omega}_t \tag{31}$$

Another object policymakers care about is the unemployment-inflation trade-off, that is, the nominal effects relative to the real effects of a monetary shock. However, state-dependence in impulse responses alone may not lead to different unemployment-inflation trade-offs, this depends on whether the real versus nominal effects differ across states. To illustrate that unemployment-inflation trade-off is state dependent, we introduce the concept of the Philips multiplier as in Barnichon and Mesters (2021) (motivated by Mankiw, 2001). The Philips

multiplier is the trade-off characterized by the average change in inflation caused by an interest rate change lowering the unemployment rate by one percentage point over h periods:

$$T_h = \frac{\partial \bar{\Pi}_{t:t+h}}{\partial R_t}\Big|_{\varepsilon_t} \Big/ \frac{\partial \bar{U}_{t:t+h}}{\partial R_t}\Big|_{\varepsilon_t}$$

Here $\bar{\pi}_{t:t+h}$ is the average over variable Π over h time periods, and ε_t is the exogenous change in the interest rates. The statistical counterpart of T_h is the so-called Philips multiplier (Barnichon and Mesters, 2021):

$$\mathcal{P}_h = \mathcal{R}_h^{\bar{\Pi}} / \mathcal{R}_h^{\bar{U}}, \quad h = 0, 1, 2, ...,$$

that is, the ratio of the sum of the impulse response function (up to horizon h) of inflation over unemployment. The Philips Multiplier can loosely be interpreted as the slope of the Philips curve. In the case of state-dependent impulse response functions, the Philips Multiplier is naturally also state-dependent.

We compute the Philips multipliers for each of the four versions of the model. In the simple model the small (large) surplus parameterizations have Philips multipliers of -0.059 (-0.148), and for the full model the Philips multipliers are -0.062 (-0.155). This gives some intuition as to why the multipliers are smaller in times of high unemployment, as the surplus is small and the real effects of monetary shocks are magnified.

4 Computation and Estimation

First, we outline our computational algorithm for the global solution to the model, given a set of parameter values. Second, we discuss the Bayesian sampler and nonlinear filter we use along with the global solution algorithm to estimate the model parameters.

4.1 Computational Algorithm

In this subsection, we elaborate on our computational algorithm. The algorithm is based on Judd et al. (2014), who use their algorithm to globally solve the multi-country real business cycle model. We describe the algorithm in the main text, because while of lower dimensionality, our policy updating rules are somewhat more complex than in their model. In addition, we deviate from their algorithm in how we deal with the exogenous states Z_t and D_t. Rather than integration, we use finite-state Markov chain approximations to deal with the exogenous states, as this is convenient for our estimation procedure detailed in the next subsection.

Our model can be cast to have four endogenous states: (R_t, N_t, V_t, Y_t), that is, interest rates, the employment stock, the vacancy stock and output. In addition, we have two exogenous states, the discount factor shock D_t and the total factor productivity shock Z_t. We need to solve for five policies functions: $g^{\Pi}(Z, D, N, R, V, Y)$ for inflation, $g^{x}(Z, D, N, R, V, Y)$ for the vacancy flow, $g^{\mu}(Z, D, N, R, V, Y)$ for the value of a job, $g^{w}(Z, D, N, R, V, Y)$ for the wage, and $g^{\omega}(Z, D, N, R, V, Y)$ the multiplier on the output constraint.

Because we discretize total factor productivity, we have $Z_t \in \mathcal{Z} = \{z_1, ..., z_{n_z}\}$ with P_z its transition probability matrix, and similar for D_t. Because of this, a policy function becomes: $g^{\cdot}_{z,d}(R, N, V)$ for each $(z, d) \in \mathcal{Z} \times \mathcal{D}$. We approximate each policy function, conditional on a discrete realization of the exogenous states, using a four-dimensional Chebychev polynomial:

$$g^{\pi}_{z,d}(R, N, V) = \sum_{i=1}^{N_R} \sum_{j=1}^{N_N} \sum_{k=1}^{N_V} \sum_{l=1}^{N_Y} c^{z,d,\Pi}_{ijkl} \phi_i(R) \phi_j(N) \phi_k(V) \phi_l(Y) \tag{32}$$

and the same for the other policy functions.

Given some initial guess for the coefficients $c^{z,d,\Pi}_{ijkl}$, $c^{z,d,w}_{ijkl}$, $c^{z,d,\omega}_{ijkl}$, $c^{z,d,x}_{ijkl}$, $c^{z,d,\mu}_{ijkl}$, using our policies, we update our states using the model equations:

$$\begin{aligned}
N' &= (1 - \delta)N + g^{q}_{z,d}(V + g^{x}_{z,d}) \\
V' &= (1 - \xi)(1 - g^{q}_{z,d})(V + g^{x}_{z,d}) \\
R' &= \left[R^* \left(\frac{g^{\pi}_{z,d}}{\Pi^*} \right)^{\psi_1} \left(\frac{ZN^{\alpha}}{Y^*} \right)^{\psi_2} \right]^{1-\rho_R} R^{\rho_R} e^{\epsilon_R} \\
\ln Z' &= \rho_z \ln Z + \sigma_z \varepsilon_z \\
\ln D' &= \rho_d \ln D + \sigma_d \varepsilon_d \\
Y' &= ZN'
\end{aligned}$$

where $g^{\theta}_{z,d} = (V + g^{x}_{z,d})/(\delta + (1 - \delta)(1 - N))$ and $g^{q}_{z,d} = \chi(1 + (g^{\theta}_{z,d})^{\iota})^{-1/\iota}$. For our exposition below, we also need to define $g^{f}_{z,d} = g^{q}_{z,d} g^{\theta}_{z,d}$. We can now evaluate our policies in N', R', V', Y', Z', D', resulting in $g^{\Pi'}_{z',d'}$, etc. Note that the timing of the model is intricate, so we also need to keep track of $N'' = (1 - \delta)N' + g^{q'}_{z',d'}(g^{x'}_{z',d'} + V')$ and $Y'' = Z'N''$.

Next, we update our policies. To do so, we first need to update the stochastic discount factor. The consumption multiplier:

$$g^{\lambda}_{z,d} = D(Y' - bY)^{-\tau}$$

and the stochastic discount factor:

$$\tilde{Q} = \beta \frac{g^{\lambda'}_{z',d'}}{g^{\lambda}_{z,d}}.$$

Our policy rule for inflation can be updated using the Euler Equation:

$$\tilde{g}^{\pi}_{z,d} = \mathbb{E}_{Z,D}\left[\tilde{Q}\frac{R'}{g^{\pi'}_{z'}} g^{\pi}_{z}\right].$$

The updating equation for the multiplier of the output constraint follows from the pricing equation:

$$\tilde{g}^{\lambda}_{z,d} = \gamma\left(1 - \phi(g^{\Pi}_{z,d} - \Pi^*)g^{\Pi}_{z,d} + \phi\mathbb{E}_{Z,D}\left[\tilde{Q}\left(g^{\Pi'}_{z',d'} - \Pi^*\right) g^{\Pi'}_{z',d'}\frac{Y''}{Y'}\right]\right).$$

The job creation condition gives an update for g^{x}_{z}:

$$\tilde{g}^{x}_{z,d} = \frac{g^{q}_{z,d} g^{\mu}_{z,d} - \kappa}{\psi_x} + (1 - g^{q}_{z,d})(1-\xi)\mathbb{E}_{Z,D}\left[\tilde{Q} g^{x}_{z',d'}\right].$$

The wage is updated using:

$$\tilde{g}^{w}_{z,d} = \nu - \left((1-\delta)\mathbb{E}_{Z,D}\left[\tilde{Q} g^{\mu'}_{z',d'}(1 - g^{q'}_{z',d'} g^{\theta'}_{z',d'})\right] - g^{\mu}_{z,d}\right)\frac{\eta}{1-\eta}.$$

The job value is updated using:

$$\tilde{g}^{\mu}_{z,d} = (1 - g^{\omega}_{z,d})Z - g^{w}_{z,d} + (1-\delta)\mathbb{E}_{Z,D}\left[\tilde{Q} g^{\mu'}_{z',d'}\right].$$

Note that the expectations are computed using the transition probability matrix for Z and D. Next, we again compute the coefficients $c^{z,d,\Pi}_{ijkl}$ etc., using a regression of the updated policy rules and the Chebychev nodes. Repeat this, by again updating the states and policies. Iterate until the convergence criterion is met. One can use damping to make the algorithm more stable.

Computational details For the grids of the state variables N, R, V, and Y, we construct ergodic sets based on the linearized solution, taking into account how the range of the variables change with Z and D. The grids don't change when updating the policies, which is a deviation from Judd et al. (2014) who iteratively update the grid to deal with the curse of dimensionality, but we choose not to, because our state space is relatively small. To discretize the stochastic

process of TFP, Z_t, and the discount factor shocks D_t, we use the Tauchen (1986) method, with 12 grid points for Z_t, and 6 grid points for D_t. We modify the transition probability matrix that follows from this discretization by correcting the transition probabilities such that the discretized process matches the conditional means of the underlying process, evaluated in each grid point. We choose a relatively large value for the number of grid points n_z because TFP is typically quite persistent, which requires more grid points, as shown in Janssens and McCrary (2022), while the estimates for the discount factor shocks show less persistence, so a lower number of grid points suffices. For moderate choices of nodes and grid sizes, the model can solve in less than 30 seconds. For more accurate solutions, the model takes several minutes to solve.

4.2 Estimation Approach

We compare the results of two estimation procedures. Both approaches use standard Bayesian estimation methods (Random Walk Metropolis Hastings Sampler) to construct the posterior distribution, and the differences between the approaches come from the solution method and filtering method. For the Random Walk Metropolis Hastings Sampler, we split the parameters in two fixed blocks: (i) structural parameters $(\eta, \nu, \xi, \kappa, \psi, \chi, \psi_1, \psi_2)$ and stochastic parameters $(\rho_r, \sigma_r, \rho_z, \sigma_z)$ and (ii) the standard deviations of the measurement error terms. This has an advantage in the global solution approach, because the model only has to be solved once per draw.

A subset of parameters is calibrated externally, being risk aversion, set to two, β is set to match the average interest rate over the sample, γ is the demand elasticity and is set to 0.1, and α is the production elasticity and is set to 1. Π_{ss} is the steady state level of inflation, fixed to 1.008385 consistent with our data sample. Furthermore, $\chi = 1$ to ensure the matching rate is a probability between 0 and 1, and we internally calibrate ι such that the steady state unemployment rate is equal to the long-run average unemployment rate for each parameter draw. η, which is the bargaining weight, is internally calibrated as to make sure the Hosios condition is satisfied, i.e., the workers' bargaining weight is equal to the elasticity of the matching functions with respect to unemployment.

The two different procedures are as follows. In the first approach, we log-linearize the NKDMP model and use the Kalman filter to evaluate its likelihood. In the second approach, we solve the model using the global method outlined in the previous subsection, initialized in the parameter estimates of the linearized model, and use a nonlinear filtering technique to evaluate the likelihood, which we use to re-estimate all parameters of interest. Both procedures use

the same sets of priors.[7] This is to ensure any differences between the estimates are driven by the solution method and sampler, and not by the prior. We elaborate on our choice for the nonlinear filter in the next subsection.

4.2.1 Nonlinear Filtering

Our estimation approach uses the discretization filter of Farmer (2021). The idea behind the discretization filter is that by approximating the state space using a discrete-valued Markov chain, the likelihood can be evaluated recursively and fast using simple matrix multiplications. This results in an approximate likelihood of nonlinear models that can be used in classical (frequentist) or Bayesian estimation procedures.

Denote the states of the model at time t by $X_{t,M}$ with M different realizations on a discrete grid, with transition probability matrix $P_{\theta,M}$ which has elements $P_{\theta,M}(m, m') = \mathbb{P}_\theta(X_{t,M} = x_{m',M}|X_{t-1,M} = x_{m,M})$. With some abuse of notation relative to the previous section, θ is a vector summarizing the parameters of the structural model. We assume $X_{t,M}$ is governed by this transition probability matrix $P_{\theta,M}$, and we have measurement equations

$$Y_t|X_{t,M} \sim g_\theta(Y_t|X_{t,m})$$

that map the unobserved states $X_{t,m}$ into observables. As is common, we assume each variable is observed with Gaussian i.i.d. measurement error relative to its model counterpart, with standard errors we estimate jointly with our other parameters.

The likelihood of the model is now easy to evaluate. Let $\hat{\zeta}_{t,M|t} = \mathbb{E}_\theta[\zeta_{t,M}|Y_1^t]$ be the vector of filtered probabilities of being in each state, using information up to time t. The forecast equation is then:

$$\hat{\zeta}_{t,M|t-1} = \mathbb{E}_\theta[\zeta_{t,M}|Y_1^{t-1}] = P'_{\theta,M}\hat{\zeta}_{t-1,M|t-1}$$

Defining $\eta_{t,M}$ as an $M \times 1$ vector containing the likelihoods of observing Y_t conditional on being at state m at time t, for $m = 1, ..., M$, the marginal likelihood of Y_t given Y_1^{t-1} is given by $p_{\theta,M}(Y_t|Y_1^{t-1}) = \mathbf{1}'(\eta_{t,M} \odot \hat{\zeta}_{t,M|t-1})$ with $\odot$ element-wise multiplication and $\mathbf{1}$ a vector of ones. We then update $\hat{\zeta}_{t,M|t} = \frac{\eta_{t,M} \odot \hat{\zeta}_{t,M|t-1}}{p_{\theta,M}(Y_t|Y_1^{t-1})}$. The log likelihood is then the sum over $t = 1, ..., T$ of the logs of the marginal likelihoods.

[7] The prior choices are in line with the existing literature, and selected to cover a reasonable parameter range and not be too influential. See, for example, prior choices in Krause and Lubik (2007), Borağan Aruoba et al. (2018), and Farmer (2021).

This method may suffer from the curse of dimensionality, in the sense that if there are many state variables X_t, M has to be large, and, given that most discretization methods rely on tensor products, $P_{\theta,M}$ quickly becomes larger than a typical computer can store. We show that for macro models featuring both exogenous and endogenous states, this issue can be partially aided. In the case of our model, recall that we have four endogenous state variables: N_t, V_t, R_t and Y_t, and two exogenous state variable: Z_t and D_t. Let N_{endo} be the number of discrete values the endogenous states can take, and N_{exo} the total number of discrete values the exogenous states can take. We have $M = N_{\text{endo}} \times N_{\text{exo}}$. For the purpose of likelihood evaluation, we only need to store P_{endo}, which is $M \times N_{\text{endo}}$, that is, the transition probability matrix of all possible states to the N_{endo} different endogenous states, and P_{exo} which is the transition probability matrix governing the exogenous variables. Define $D = I_{N_{\text{exo}}} \otimes \mathbf{1}_{1\times N_{\text{endo}}}$ and $B = P'_{\text{exo}} D$. Here $I_{N_{\text{exo}}}$ is an identity matrix of size N_{exo}. We can update our forecast ζ in two steps:

$$F_{t-1} = P_{\text{endo}} \cdot \hat{\zeta}_{t-1,M|t-1}$$

and

$$\hat{\zeta}_{t,M|t-1} = F'_{t-1} B'.$$

Using this two-step update allows us to use more grid points and therefore get a better approximation of the likelihood. In particular, we will use 12 grid points for our exogenous variable Z_t, and 6 for D_t, consistent with our computation approach, 9 grid points to discretize N, 7 grid points to discretize V, and 5 grid points to discretize R and 5 grid points for Y. To construct P_{endo}, we use the policy rules to compute next period's states, and let P_{endo} be a weighted probability of the distance of next period's state to the grid points. To construct our grids for N, V and R and Y, we use the same grid widths as used in the global model solution, which we pick to be slightly wider than the ergodic sets from the linearized solution.

As shown in Farmer (2021), most of the computation time of the discretization filter goes to the construction of the discrete Markov chains. However, as explained in the previous subsection, our computational approach already relies on a discretization of the exogenous variables, and the transition dynamics for the other states and variables are easy to compute and follow directly from the computed policy rules. As such, the discretization filter can be used to compute (an approximation of) the likelihood of our model with little additional cost once the model has been solved. This is an important advantage compared to particle filters used by for example, Gust et al. (2017), to estimate a globally solved model. In their application, the

computational costs for solving the model and evaluating the likelihood are of the same order of magnitude.[8]

4.3 Data

Data used for estimation are summarized in Table A2 in the Appendix. This description also includes the data transformations used. In particular, we use the Hamilton filter (2018) to remove long-run trends. Our five variables of interest are: the unemployment rate, output per worker, market tightness, the federal funds rate and inflation. We consider the period 1967-2019, with a quarterly frequency.

5 Comparing the Linear and Nonlinear NKDMP Model

In this section, we asses the differences between the linear and global model solution. First, we present and compare the estimation results. Next, we compare the differences in model dynamics and distributions.

5.1 Comparing Estimation Results

Table 1 summarizes the model parameters, the prior selection, and the parameter estimates for the linearized NKDMP model and the NKDMP model solved using global projection methods. We use the same priors for the linearized and nonlinear model to ensure differences in posteriors are driven by the model solution method and not by the prior choice. We initialize the sampler of the global model parameters at the posterior mean of the linearized model parameter estimates.

From Table 1, we see there are some important differences between the local and global parameter estimates. The following parameters stand out and are particularly important for the model dynamics. First, the outside option ν is lower in the global model estimation than in the linearized model, and the posterior mode decreases from 0.85 to around 0.81. The outside option ν is important for the labor market dynamics and volatility. Given that – as we will see below – the global model solution is more volatile than the linearized solution for the same parameters, it is sensible that ν is lower in the global estimation procedure. Similarly, we see decreases in the variances of the exogenous shocks, given by σ_z and σ_d. Second, as the outside option ν decreases, the vacancy costs have to increase as to match the market tightness in the

[8] Admittedly, the model in Gust et al. (2017) has a larger state space and it would therefore likely be infeasible to use the discretization filter to estimate it, even after using our proposed two-step decomposition of exogenous and endogenous states.

Table 1: Parameters, priors (mean and std), posterior (mean, standard deviation in brackets) of linearized model, and global model solution.

Param.	Description	Prior	Linear		Global	
		Calibration				
α	Production elasticity	-	1.0		1.0	
β	Discount factor	-	0.9926		0.9926	
γ	Demand elasticity	-	0.10		0.10	
δ	Separation rate	-	0.1		0.1	
τ	Risk aversion	-	2.0		2.0	
		Estimation structural parameters				
ϕ	Price adjustment cost	G(20,5)	70.58	(8.996)	69.57	(6.256)
ν	Outside option of the worker	B(0.45,0.01)	0.849	(0.008)	0.809	(0.005)
ξ	Vacancy depreciation rate	B(0.2,0.1)	0.185	(0.034)	0.218	(0.041)
κ	Vacancy maintenance cost	G(0.5,0.1)	0.036	(0.008)	0.076	(0.005)
ψ_x	Vacancy creation cost	G(0.5,0.1)	0.233	(0.047)	0.297	(0.031)
b	Habit parameter	B(0.7,0.15)	0.802	(0.042)	0.741	(0.026)
ψ_1	Taylor rule weight inflation	G(1.5,0.5)	2.221	(0.228)	2.472	(0.232)
ψ_2	Taylor rule weight output gap	G(0.25,0.1)	0.359	(0.080)	0.436	(0.050)
ρ_r	Inertia of Taylor rule	B(0.6,0.2)	0.888	(0.015)	0.770	(0.017)
σ_r	Standard deviation MP shocks	IG(0.3,4)	0.002	(0.0001)	0.002	(0.0002)
ρ_z	Persistence of TFP shocks	B(0.6,0.2)	0.964	(0.021)	0.951	(0.003)
σ_z	Standard deviation TFP shocks	IG(0.3,4)	0.003	(0.001)	0.002	(0.0001)
ρ_d	Persistence of DF shocks	B(0.6,0.2)	0.725	(0.054)	0.669	(0.041)
σ_d	Standard deviation DF shocks	IG(0.3,4)	0.043	(0.007)	0.019	(0.0004)
		Estimation measurement errors standard deviations				
$\sigma_{\text{ME}}^{\theta}$	Measurement Error θ	IG(0.5,5)	0.081	(0.009)	0.099	(0.010)
σ_{ME}^{Π}	Measurement Error Π	IG(0.5,5)	0.002	(0.0001)	0.006	(0.0003)
σ_{ME}^{OPW}	Measurement Error Y/N	IG(0.5,5)	0.022	(0.001)	0.022	(0.001)
σ_{ME}^{U}	Measurement Error U	IG(0.5,5)	0.078	(0.005)	0.078	(0.005)
σ_{ME}^{R}	Measurement Error R	IG(0.5,5)	0.001	(0.0001)	0.002	(0.0002)

Notes: **These estimates are very preliminary**. If there are no standard errors in between brackets, it means that the parameters are calibrated/fixed instead of estimated. G stands for the Gamma distribution, B for Beta, IG for inverse-Gamma. Linearized model estimates are based on 300,000 draws from a block Random-Walk-Metropolis-Hasting sampler using the Kalman filter, with a burn-in of 100,000 draws. The global parameters are based on 12,000 draws, after 6,000 burnin (over 4 chains).

data, which is why the global model solution has higher values for vacancy-related costs κ and ψ_x. Third, the posterior mode of ρ_r, the persistence of the Taylor rule, is lower in the global model estimation than in the linearized model estimates. This difference comes from the fact that in the global (nonlinear) model, the interest rate is bounded below by zero but governed by an unbounded shadow rate. Because of the fairly long zero-lower-bound episode in the

data, the linear model interprets this as a highly inertial interest rate rule, while the nonlinear model understands that the shadow rate may have moved while the actual policy rate was stuck at the zero lower bound. Fourth, we find that both Taylor rule weights increase.

5.2 Comparing Ergodic Sets

In this section, we compare ergodic sets as simulated from the linearized NKDMP model with those from the global model solution. In Figure 5, we visualize the ergodic distributions from both model solutions, evaluated at the parameters in Table 1 in the column "global", which corresponds to the mean of the global model posteriors. As can be seen, the two model solutions, when evaluated in the same parameters, result in considerably different ergodic sets. This is consistent with the findings of Petrosky-Nadeau and Zhang (2017) for the DMP model, but the large differences in the nominal variables suggest that New Keynesian model elements introduces important additional nonlinearities.

Figure 5 shows that for the same parameters, the global model solution generates more volatility in most variables: unemployment has a range of 3.5%-9% in the global model solution, while the linearized solution ranges from 4%-7% for the same set of parameters, explaining why we find a lower outside option value ν in our global estimation procedure. The figure also suggests a stronger correlation between TFP (Z) and unemployment, vacancies and tightness in the global model solution than in the linearized solution. Inflation, on the other hand, is less correlated with TFP than in the linearized model.

The ergodic sets of the linear model *evaluated in the linear parameter estimates* are shown in Appendix C. The large differences between the ergodic sets of the two linear models (evaluated in the linear and global parameter estimates, respectively) are another dimension illustrating the sizeable differences between the two sets of parameters reported in Table 1.

5.3 Comparing Model Dynamics

Next, we compare the differences in model dynamics between the linearized and global model, by evaluating and comparing the impulse response functions to a TFP shock and a monetary policy shock. For this exercise, we focus on dynamics around the steady state. Dynamics away from the steady state, and particularly, state-dependence, will be the focus of the next section.

Figure 6 shows the response to a 40 basis point shock to the interest rate, for the global and linearized model. As we can see, in the global model solution, employment is about twice

Figure 5: Ergodic distributions for the linearized (red) and global (blue) NKDMP model

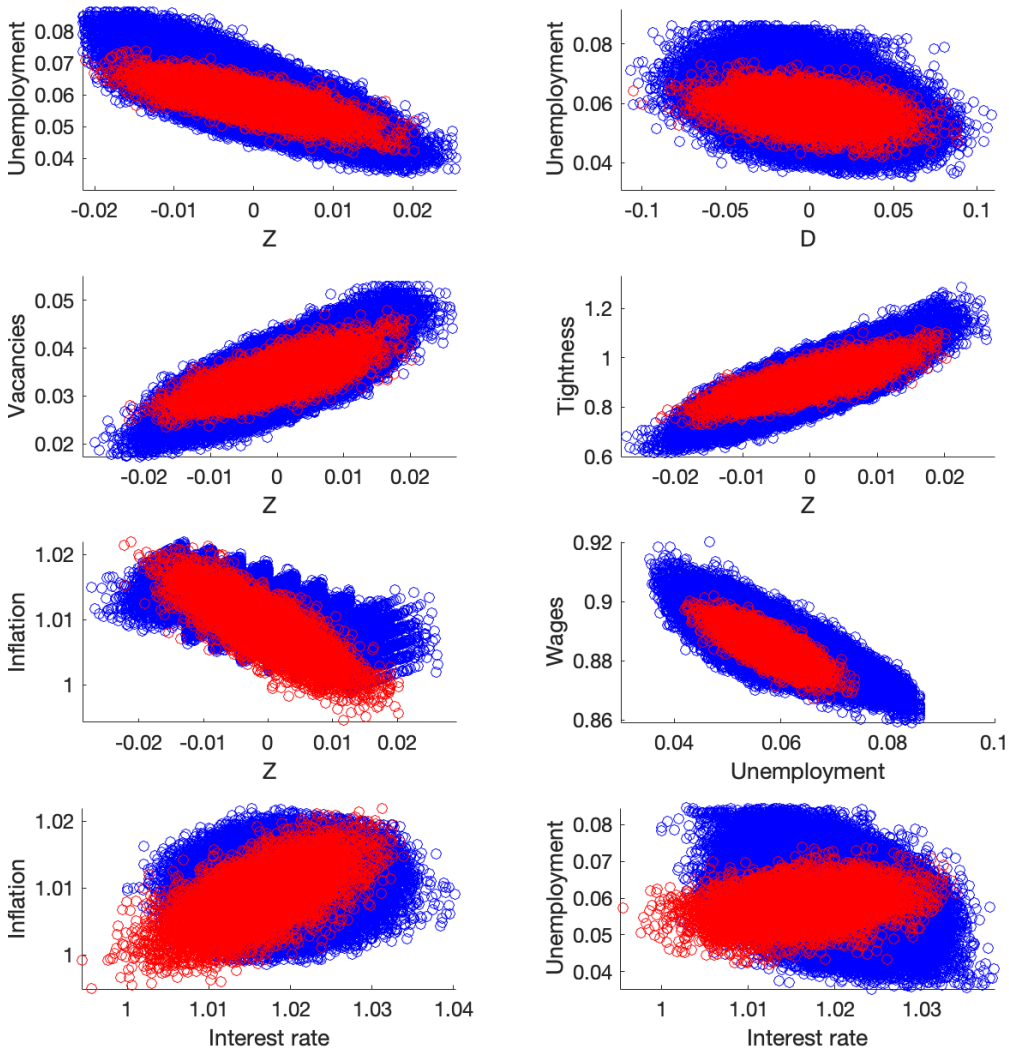

Notes: Based on parameter estimates of the global model solution, summarized in Table 1. The global model solution in this figure uses $N_N = 3, N_R = 3, N_V = N_Y = 2$, and uses 10 grid points for Z, and 6 for D.

as responsive, and also the initial response for inflation is larger. Note that our steady-state impulse response functions are quite comparable to the baseline empirical evidence in Figure 1: the peak response of the global model for employment is around -0.12, as in the local projections. The peak response of vacancies in the model and data (Help-Wanted-Index) are both around -2%. Also the response of market tightness falls well within the empirical confidence intervals of our baseline local projection specification. For comparison, the impulse

response functions of the linear model evaluated in the linear parameter estimates are shown in Figure C2 in the Appendix.

Figure 6: Impulse Response Functions to a 40bp MP shock for the linearized (red line) and global NKDMP model

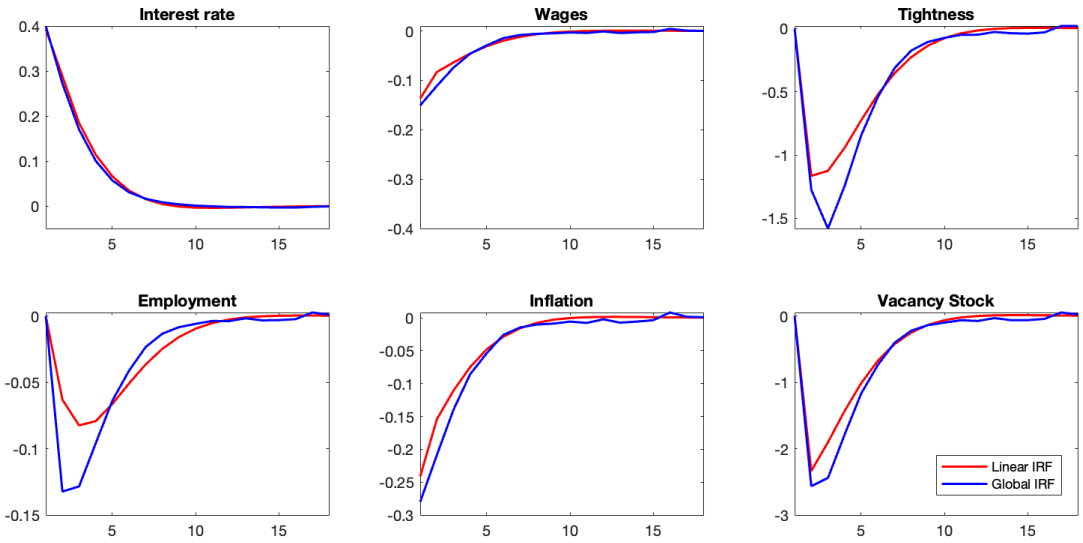

Notes: Based on parameter estimates of the global model solution, summarized in Table 1.

Figure 7 shows the response (around steady state) to a positive TFP shock of 0.005, for the linear and global model evaluated in the global parameter estimates. The differences between the global and linear model solution are large. For the global model, we find that real variables (employment, tightness, vacancies) are about twice as responsive than in the linear model. Nominal variables (inflation, interest rate, wages), on the other hand, are less responsive in the global model than in the linearized model solution.

Figure 7: Impulse Response Functions to a 50bp TFP shock for the linearized (red line) and global NKDMP model (blue solid line).

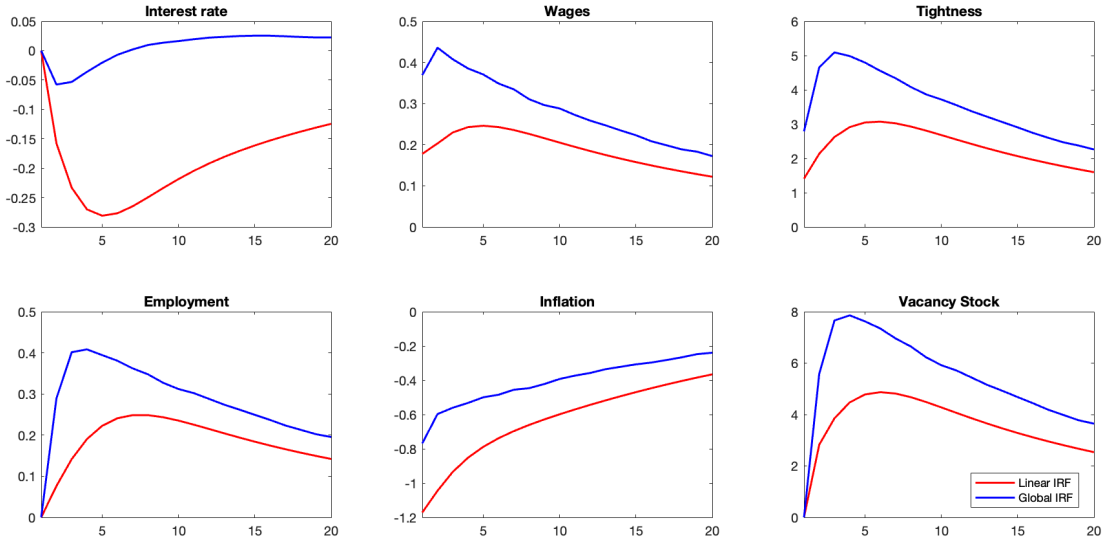

Notes: Based on parameter estimates of the global model solution, summarized in Table 1.

6 State-Dependence in the NKDMP model

6.1 Filtering Time-varying Impulse Response Functions

While the previous section demonstrates that the linearized model and global model solutions differ substantially in their dynamics and implied parameter estimates, our main motivation for using a global solution approach is its ability to generate state-dependent impulse response functions, which is the focus of this section. In particular, in the global model solution, the policy, given by Equation (31), differs for each value of the endogenous variables N, R, V, Y and exogenous variables Z and D. Rather than evaluating the policies in an arbitrary choice of states, in this section, we use our nonlinear filter (the discretization filter of Farmer (2021) in combination with our global solution approach) to filter these underlying states of the economy, and evaluate the policies of our global model solution to construct a time-varying impulse response function at each point in time.

Figure 8 shows the impulse response functions to a 40bp monetary policy shock at each point in time from 1967 to 2019 based on the filtered states and global model solution. The figure shows that the impulse response function for inflation does not vary strongly over time, consistent with our empirical evidence, although the inflation response pre-2000 was more persistent than post-2000. In contrast, the impulse response function of employment varies strongly over time, with countercyclical size and persistence: the effects of a monetary policy shock on employment are larger and longer-lasting during recessions (high unemployment) than expansions (low unemployment). This is most visible for the recessions before the 2000's, while the figure show that impulse response functions post 2000's show smaller and less persistent effects. The time-varying impulse response functions for wages, tightness and vacancies show similar patterns as for employment.

Figure 8: Time-Varying Impulse Response Functions to a 40bp MP shock for the global NKDMP model.

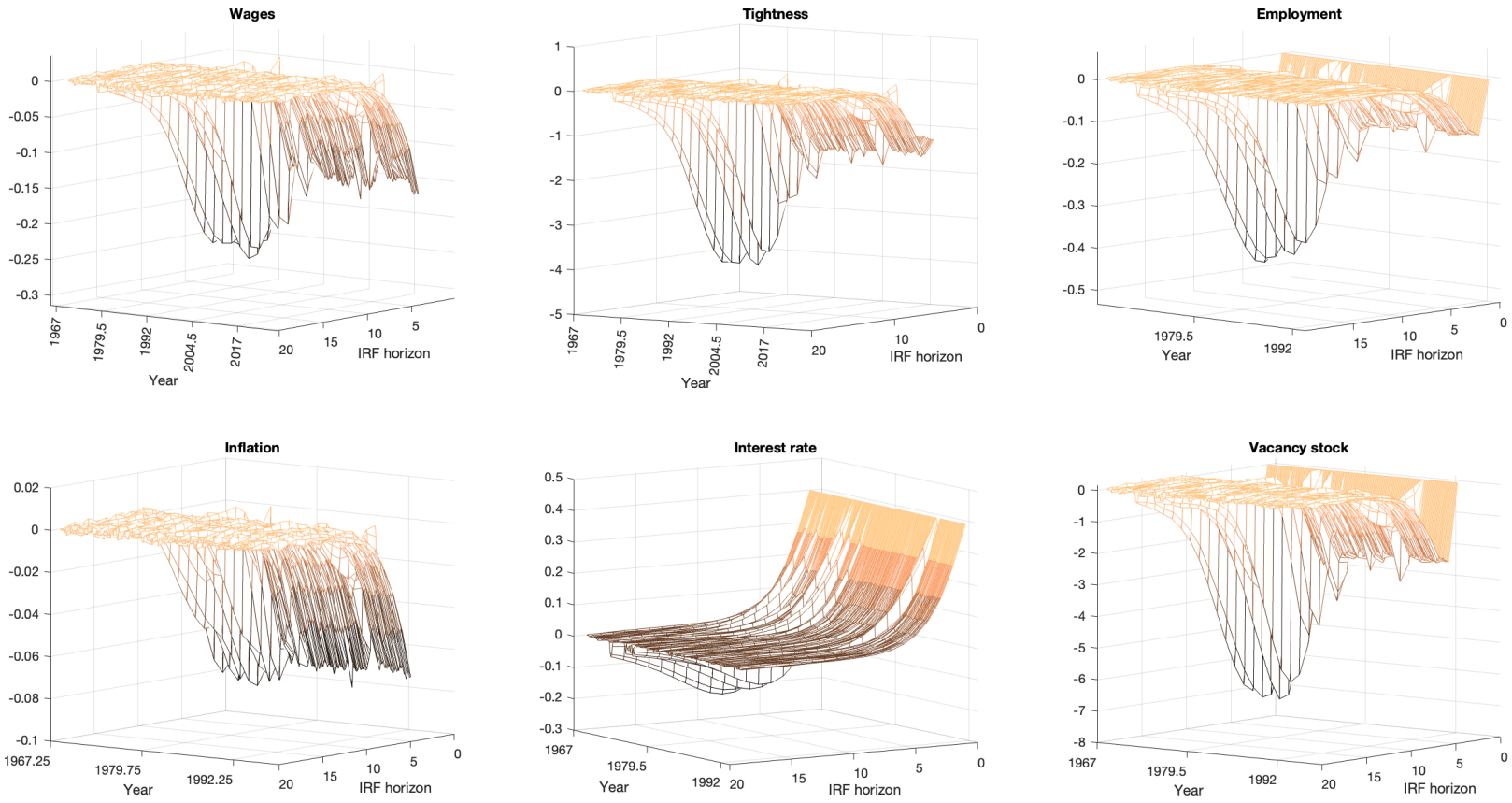

Notes: Based on parameter estimates of the global model as summarized in the last column of Table 1.

6.2 Drivers of State-Dependence

Next, we ask what the main drivers of state-dependence in our NKDMP model are? As described in Section 3, a shock to the interest rate has highly nonlinear effects on labor demand through the flow profit of the firm, and as such, the value of a job μ_t. A shock to the marginal costs has large effects when output and employment are low, relative to when output is high. Similarly, when interest rates are high, increasing them even more has a larger effect than when interest rates were low to begin with. We verify this mechanism in the estimated global model as shown in Figure 9, where we plot impulse response functions of μ_t to a 40bp monetary policy shock. When interest rates are low, there is little state-dependence in unemployment. When interest rates are high, a shock to the interest rate has stronger effect when in a high than in a low unemployment environment.

Figure 9: Impulse Response Functions of μ (the value of a job) to a 40bp MP shock for the global NKDMP model.

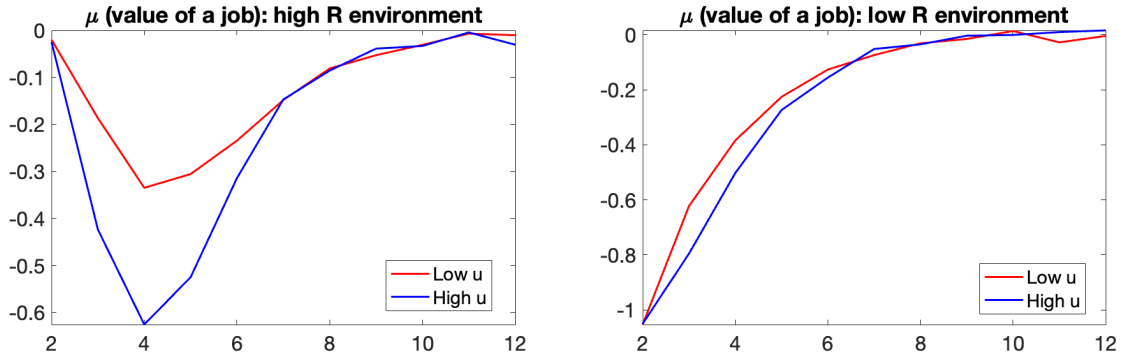

Notes: Based on parameter estimates of the global model as summarized in the last column of Table 1. High interest rate: 1.036, low interest rate: 1.01, low unemployment: 3.8%, high unemployment: 8.8%.

Figure 9 also helps us understand the time-variability we observe in the impulse response functions in Figure 8. In particular, we see that most time-variability occurs in the first half of the sample (pre-2000's), while the impulse response functions in the second half of the sample vary less. This is because the interest rate in the second half of the sample is considerably lower than in the first half, and, as Figure 9 shows, state-dependence in unemployment is strongest in high interest rate environments.

6.3 A State-Dependent Philips Multiplier

What are the policy implications of state-dependent impulse response functions? One statistic that policy makers, in particular, central banks, care about is the trade-off between inflation and unemployment, loosely interpretable as the slope of the Philips curve. Figure 10 visualizes

the Philips Multiplier based on the global NKDMP model, four years after shock impact. We see that the Philips Multiplier is strongly procyclical, which, informally, means that the Philips curve is considerably flatter during recessions than expansions. The Philips Multiplier has a baseline value (i.e., in "normal times") of -0.1. In bad times, for example during the recessions in the 70's and 80's, the Philips Multiplier peaks to around -0.05, i.e., about half. The Philips Multiplier of the linearized model is constant, and, when evaluated in the linear parameter estimates of Table 1, is equal to -0.09 after four years, suggesting the linearized model captures the average Philips Multiplier accurately.

Comparison with other empirical evidence on the Philips Multiplier In the local projection estimates from Figure 2, we find a Philips Multiplier after four years of -0.1. With the effects of state-dependence, we find that when we are in the 60th quantile (high unemployment), the multiplier goes up to -0.06, suggesting these estimates are fairly comparable, but quite a bit stronger. Looking at the existing literature, our baseline estimate of -0.1 is consistent with Barnichon and Mesters (2021) post-1990's estimate, and the estimates of Hazell et al. (2022). The range of our estimates is comparable to Gitti (2024), who posits that the Philips curve is nonlinear in market tightness,[9] and finds a multiplier of -0.03 when markets are slack, versus -0.08 when markets are tight.

Figure 10: Philips Multiplier based on Time-Varying Impulse Response Functions to a 40bp MP shock for the global NKDMP model.

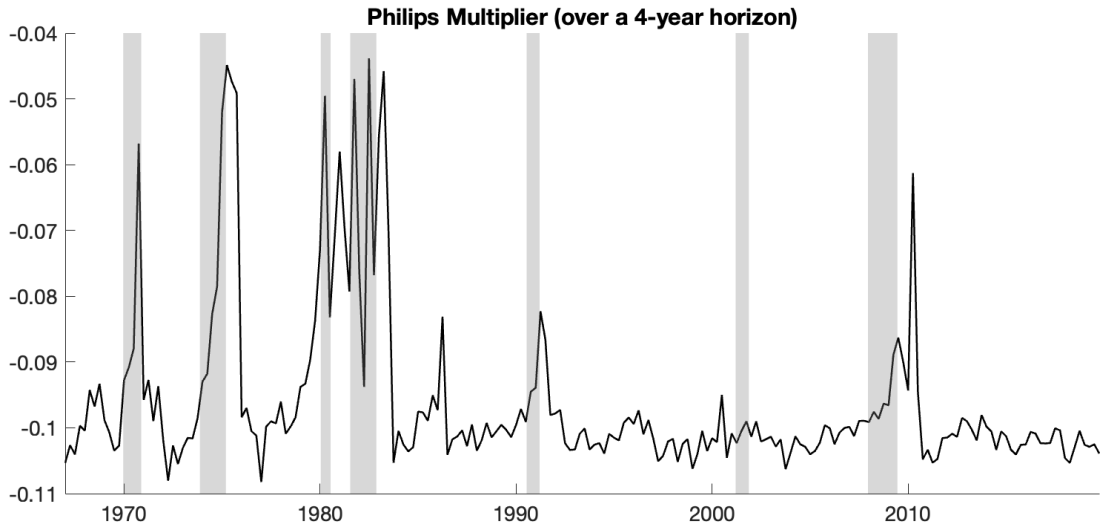

Notes: Based on global parameter estimates summarized in Table 1 and nonlinear filter of the underlying states.

[9]By assuming there is a kink in the Philips curve at market tightness $\theta = 1$

Figure 11: Impulse Response Functions to a negative 40bp MP shock during the Zero Lower Bound (2010Q2)

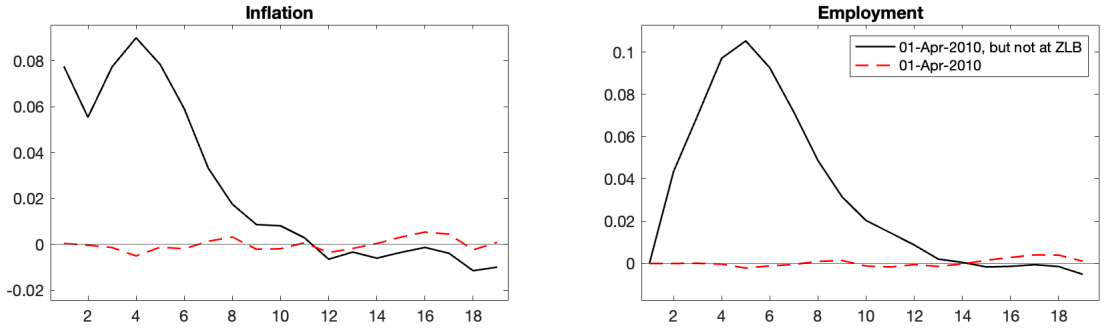

6.4 Zero Lower Bound

Next, we use our time-varying impulse response functions to study two specific periods in time. First, the zero-lower-bound period after the great financial crises, and, in the next subsection, the so-called “soft-landing" in 2022, post-pandemic.

Figure 10 shows a peak in the Philips Multiplier in 2010Q2, yet we do not see a large employment impulse response function around that time in Figure 8. We use the filtered states that come out of our estimation procedure, and compute the impulse response functions to a *negative* 40bp monetary policy shock. This is visualized by the red-dashed line in Figure 11. As can be seen, the impulse response functions during the ZLB were essentially flat. This is why the Philips Multiplier peaked around that time; we were (almost) dividing zero by zero.

We can also use our model to analyze the following counterfactual: what if in 2010Q1 the interest rate was not yet at 0, but at 1%, and we would have a -40bp monetary policy shock? The shock would have had a small but positive effect of inflation, and also boosted employment. To contrast this with the linear model, the impulse response functions always look like Figure C2, independent of the underlying states of the economy, as such largely overstating the effects lowering interest rates would have had at that time.

6.5 Soft Landing

Our model and estimates also relate to the recent “Soft Landing” discussion, see e.g., Boocker and Wessel (2023), where the big question was whether central banks would be able to increase interest rates to tame the post-pandemic inflation surge without causing large increases in the unemployment rate, and potentially triggering a recession.

Figure 12: Impulse Response Functions to a 40bp MP shock at three different dates: 2022Q2, 1975Q2, and 1980Q2.

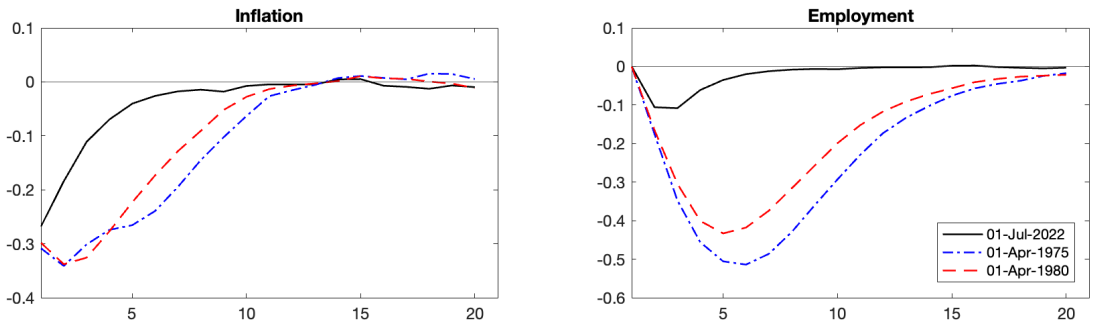

To study the Soft Landing, we extend our data set, filter the data until 2023, and compute the implied impulse response functions in 2022Q3, during which the Federal Funds Rate was increased multiple times. We contrast these impulse response functions with those computed for 1975Q2, and 1980Q2, two periods where we also saw an increase in the federal funds rate. Notably, during these periods, interest rates were high, the Philips Multiplier was high (i.e., the curve was flat, see Figure 10), and the unemployment rate was high (8.6 and 6.9, respectively, while in 2022Q3 it was 3.5). The three sets of impulse response functions are given in Figure 12. The Philips Multipliers (four-year horizon) at these specific dates were: -0.10, -0.05 and -0.05 respectively for 2022Q3, 1975Q2 and 1980Q2. As we can see from Figure 12, a positive shock to the interest rate had very small effects on employment during 2022Q3, while lowering inflation. These impulse response functions and Philips Multipliers are a plausible explanation as to why the interest rate increases during the 2022's had little effect on the US unemployment rate.[10]

7 Conclusion

The paper provided model-free estimates of the dependence the real response of identified monetary shock on the unemployment rate. We proposed a New Keynesian model with labor market frictions, and showed it can generate state-dependent impulse response functions and Philips multipliers consistent with empirical evidence identified monetary policy shocks. A global model solution and nonlinear estimation procedure expose the strong non-linearities inherent in the model, and preserves its state-dependent nature, while a linear model solution and estimation method generate different model dynamics, and fail to match empirical evi-

[10] At least as of March, 2024.

dence. Overall we find evidence and theory point to the real effects of monetary policy being larger when unemployment is high.

On the methodological side, we show that using the discretization filter of Farmer (2021), in combination with a global model solution, results in a (relatively) fast evaluation of the likelihood of our globally solved model, and allows for filtering our data, such that we can construct time-varying impulse response functions that can be used to measure the state-dependent effects of monetary policy at any point in time. Particularly, we show our model endogenously generates Philips Multipliers (i.e., inflation-unemployment trade-off) that were two times as large in expansions than during the recessions pre-1990's. A linearized solution does not feature state-dependence, and underestimates the costs of fighting inflation during high unemployment episodes.

In line with existing literature, for example, Gust et al. (2017), our paper stresses the importance of solving models using global rather than perturbation methods, and of estimating the nonlinear model rather than relying on calibration or the perturbed model estimates. We hope by showing that the combination of the discretization filter with a global model solution results in faster filtering than traditional nonlinear filters such as the particle filter, making estimation of small-scale NK models feasible on standard desktop computers, more researchers will employ these methods, and will better explore the inherent nonlinearities in these models.

References

Ahn, H. J., and Hamilton, J. D. (2022). "Measuring labor-force participation and the incidence and duration of unemployment". *Review of Economic Dynamics*, *44*, 1-32.

Angrist, J. D., Jordà, Ò., and Kuersteiner, G. M. (2018). "Semiparametric Estimates of Monetary Policy Effects: String Theory Revisited". *Journal of Business & Economic Statistics*, *36*(3), 371–387.

Barnichon, R., and Brownlees, C. (2019). "Impulse Response Estimation by Smooth Local Projections". *Review of Economics and Statistics*, *101*(3), 522–530.

Barnichon, R., Debortoli, D., and Matthes, C. (2022). "Understanding the Size of the Government Spending Multiplier: It's in the Sign". *The Review of Economic Studies*, *89*(1), 87–117.

Barnichon, R., and Matthes, C. (2018). "Functional Approximation of Impulse Responses". *Journal of Monetary Economics*, *99*, 41–55.

Barnichon, R., and Mesters, G. (2021). "The Phillips Multiplier". *Journal of Monetary Economics*, *117*, 689–705.

Benigno, P., and Eggertsson, G. B. (2023). *"It's baaack: The Surge in Inflation in the 2020s and The return of the Non-Linear Phillips Curve"* (Tech. Rep.). National Bureau of Economic Research.

Ben Zeev, N., Ramey, V. A., and Zubairy, S. (2023). "Do Government Spending Multipliers Depend on the Sign of the Shock?". In *AEA Papers and Proceedings* (Vol. 113, pp. 382–387).

Blanchard, O. (2016). "The Phillips Curve: Back to the'60s?". *American Economic Review*, *106*(5), 31–34.

Blanchard, O., and Galí, J. (2010). "Labor markets and monetary policy: A new keynesian model with unemployment". *American economic journal: macroeconomics*, *2*(2), 1–30.

Boocker, S., and Wessel, D. (2023). *"Brookings Commentary: What is a Soft Landing?"*. Retrieved from https://www.brookings.edu/articles/what-is-a-soft-landing/ (Accessed on March 20, 2024)

Borağan Aruoba, S., Cuba-Borda, P., and Schorfheide, F. (2018). "Macroeconomic Dynamics near the ZLB: A Tale of Two Countries". *The Review of Economic Studies*, *85*(1), 87–118.

Calvo, G. A. (1983). "Staggered Prices in a Utility-Maximizing Framework". *Journal of Monetary Economics*, *12*(3), 383–398.

Cerrato, A., and Gitti, G. (2022). "Inflation Since Covid: Demand or Supply". *Available at SSRN 4193594*.

Christiano, L. J., Eichenbaum, M. S., and Trabandt, M. (2016). "Unemployment and Business Cycles". *Econometrica*, *84*(4), 1523–1569.

Cloyne, J., Jordà, Ò., and Taylor, A. M. (2023). *"State-Dependent Local Projections: Understanding Impulse Response Heterogeneity"* (Tech. Rep.). National Bureau of Economic Research.

Coibion, O., and Gorodnichenko, Y. (2015). "Is the Phillips Curve Alive and Well After All? Inflation Expectations and the Missing Disinflation". *American Economic Journal: Macroeconomics*, *7*(1), 197–232.

Diamond, P. A. (1982). "Wage Determination and Efficiency in Search Equilibrium". *The Review of Economic Studies*, *49*(2), 217–227.

El-Shagi, M. (2019). "A Simple Estimator for Smooth Local Projections". *Applied Economics Letters*, *26*(10), 830–834.

Farmer, L. E. (2021). "The Discretization Filter: A Simple Way to Estimate Nonlinear State Space Models". *Quantitative Economics*, *12*(1), 41–76.

Fernald, J. (2014). "A Quarterly, Utilization-Adjusted Series on Total Factor Productivity"..

Fernàndez-Villaverde, J., Gordon, G., Guerrùn-Quintana, P., and Rubio-Ramìrez, J. F. (2015). "Nonlinear Adventures at the Zero Lower Bound". *Journal of Economic Dynamics & Control*, *57*, 182-204.

Gali, J. (2015). *Monetary policy, inflation, and the business cycle: An introduction to the new keynesian framework and its applications* (2nd ed.). Princeton University Press.

Galí, J., Smets, F., and Wouters, R. (2012). "Unemployment in an estimated New Keynesian model". *NBER macroeconomics annual*, *26*(1), 329–360.

Gertler, M., and Karadi, P. (2015). "Monetary Policy Surprises, Credit Costs, and Economic Activity". *American Economic Journal: Macroeconomics*, *7*(1), 44–76.

Gertler, M., Sala, L., and Trigari, A. (2008). "An Estimated Monetary DSGE Model with Unemployment and Staggered Nominal Wage Bargaining'. *Journal of Money, Credit and Banking*, *40*(8), 1713–1764.

Gitti, G. (2024). "Nonlinearities in the Regional Phillips Curve with Labor Market Tightness".

Gonçalves, S., Herrera, A. M., Kilian, L., and Pesavento, E. (2023). "State-Dependent Local Projections".

Gust, C., Herbst, E., López-Salido, D., and Smith, M. E. (2017). "The Empirical Implications of the Interest-rate Lower Bound". *American Economic Review*, *107*(7), 1971–2006.

Hamilton, J. D. (2018). "Why You Should Never Use the Hodrick-Prescott Filter". *Review of Economics and Statistics*, *100*(5), 831–843.

Harding, M., Lindé, J., and Trabandt, M. (2022). "Resolving the Missing Deflation Puzzle". *Journal of Monetary Economics*, *126*, 15–34.

Harding, M., Lindé, J., and Trabandt, M. (2023). "Understanding Post-Covid Inflation Dynamics". *Journal of Monetary Economics*.

Hazell, J., Herreno, J., Nakamura, E., and Steinsson, J. (2022). "The Slope of the Phillips Curve: Evidence from US States". *The Quarterly Journal of Economics*, *137*(3), 1299–1344.

Janssens, E. F., and McCrary, S. (2022). "Finite-State Markov-Chain Approximations: A Hidden Markov Approach". *Available at SSRN 4137592*.

Jordà, Ò. (2005). "Estimation and Inference of Impulse Responses by Local Projections". *American Economic Review*, *95*(1), 161–182.

Judd, K. L., Maliar, L., and Maliar, S. (2017). "Lower Bounds on Approximation Errors to Numerical Solutions of Dynamic Economic Models". *Econometrica*, *85*(3), 991–1012.

Judd, K. L., Maliar, L., Maliar, S., and Valero, R. (2014). "Smolyak Method for Solving Dynamic Economic Models: Lagrange Interpolation, Anisotropic Grid and Adaptive Domain". *Journal of Economic Dynamics and Control*, *44*, 92–123.

Krause, M. U., and Lubik, T. A. (2007). "The (ir) relevance of real wage rigidity in the New Keynesian model with search frictions". *Journal of Monetary Economics*, *54*(3), 706–727.

Lahcen, M. A., Baughman, G., Rabinovich, S., and van Buggenum, H. (2022). "Nonlinear Unemployment Effects of the Inflation Tax". *European Economic Review*, *148*, 104247.

Ljungqvist, L., and Sargent, T. J. (2017). "The Fundamental Surplus". *American Economic Review*, *107*(9), 2630–2665.

Mankiw, N. G. (2001). "The Inexorable and Mysterious Tradeoff Between Inflation and Unemployment". *The Economic Journal*, *111*(471), 45–61.

Mortensen, D. T. (1982). "Property Rights and Efficiency in Mating, Racing, and Related Games". *The American Economic Review*, *72*(5), 968–979.

Petrosky-Nadeau, N., and Zhang, L. (2017). "Solving the Diamond–Mortensen–Pissarides Model Accurately". *Quantitative Economics*, *8*(2), 611–650.

Phillips, A. W. (1958). "The Relation between Unemployment and the Rate of Change of Money Wage Rates in the United Kingdom, 1861-1957". *Economica*, *25*(100), 283–299.

Pissarides, C. A. (1985). "Short-run Equilibrium Dynamics of Unemployment, Vacancies, and Real Wages". *American Economic Review*, *75*(4), 676–690.

Ramey, V. A. (2016). "Macroeconomic Shocks and Their Propagation". *Handbook of Macroeconomics*, *2*, 71–162.

Ravn, M. O., and Sola, M. (2004). "Asymmetric Effects of Monetary Policy in the United States". *Review-Federal Reserve Bank of Saint Louis*, *86*, 41–58.

Romer, C. D., and Romer, D. H. (2004). "A New Measure of Monetary Shocks: Derivation and Implications". *American Economic Review*, *94*(4), 1055–1084.

Rotemberg, J. J. (1982). "Sticky prices in the United States". *Journal of Political economy*, *90*(6), 1187–1211.

Smith, S., Timmermann, A., and Wright, J. H. (2023). *"Breaks in the Phillips Curve: Evidence from Panel Data"* (Tech. Rep.). National Bureau of Economic Research.

Tauchen, G. (1986). "Finite State Markov-Chain Approximations to Univariate and Vector Autoregressions". *Economics letters*, *20*(2), 177–181.

Tenreyro, S., and Thwaites, G. (2016). "Pushing on a String: US Monetary Policy is Less Powerful in Recessions". *American Economic Journal: Macroeconomics*, *8*(4), 43–74.

Thomas, C. (2011). "Search frictions, real rigidities, and inflation dynamics". *Journal of Money, Credit and Banking*, *43*(6), 1131–1164.

Wieland, J. F., and Yang, M.-J. (2020). "Financial Dampening". *Journal of Money, Credit and Banking*, *52*(1), 79–113.

Supplementary Appendix to "Unemployment and the State-Dependent Effects of Monetary Policy"

Eva F. Janssens & Sean McCrary

May 14, 2024

A Data

Table A1: Data details: local projections

Variable	Details	Transformation	Source
Unemployment Rate	Percent, Monthly, Seasonally Adjusted	None	LNS14000000
Wages	Average Hourly Earnings of Production and Nonsupervisory Employees, Total Private, Dollars per Hour, Monthly, Seasonally Adjusted	$100 \times \log$	CES0500000008
Federal Funds Rate	Percent, Monthly, Not Seasonally Adjusted	None	DFF
Market tightness	Vacancy over unemployments	$100 \times \log$	Barnicon (2010) & FRED
Job finding rate		$100 \times \log$	Shimer (2005)
CPI	Consumer Price Index for All Urban Consumers: All Items in U.S. City Average, Index 1982-1984=100, Monthly, Seasonally Adjusted	$100 \times \log$	CPIAUCSL
PPI	Producer Price Index by Commodity: All Commodities, Index 1982=100, Monthly, Not Seasonally Adjusted	$100 \times \log$	PPIACO
IPI	Industrial Production: Total Index, Index 2017=100, Monthly, Seasonally Adjusted	$100 \times \log$	IP.B50001.S
HWI	Help-Wanted-Index from Barnicon (2010), JOLTS post 2001	$100 \times \log$	Barnicon (2010)
TFP	1 quarter moving average of TFP growth	None	Fernald (2014)

Table A2: Data details: estimation and filtering

Variable	Details	Transformation	Source
Unemployment Rate	Percent, Quarterly, Seasonally Adjusted	Detrended*	UNRATE (FRED)
Average Weekly Earnings of Production and Nonsupervisory Employees Total Private	Dollars per Week, Quarterly, Seasonally Adjusted	Detrended* & demeaned	CES0500000030 (FRED)
Nonfarm Business Sector: Output per Worker	Index 2017=100 Quarterly Seasonally Adjusted	Detrended* & demeaned	PRS85006163
Market tightness	Vacancy over unemployments	Detrended*	Barnicon (2010) & FRED
Federal Funds Effective Rate	Percent	Quarterly**	DFF
CPI	Consumer Price Index for All Urban Consumers: All Items in U.S. City Average Index 1982-1984=100, Monthly, Seasonally Adjusted	Quarter-to-quarter % ch., detrended*	CPIAUCSL

Notes: (*): we use the Hamilton filter to remove long-run trends (Hamilton, 2018). (**) DFF converted to a quarterly interest rate $(100 * ((1 + DFF/100)^{(1/4)} - 1))$.

B Additional results for the Local Projections

Figure A1: State-Dependent Impulse Response Functions using Romer-Romer shocks

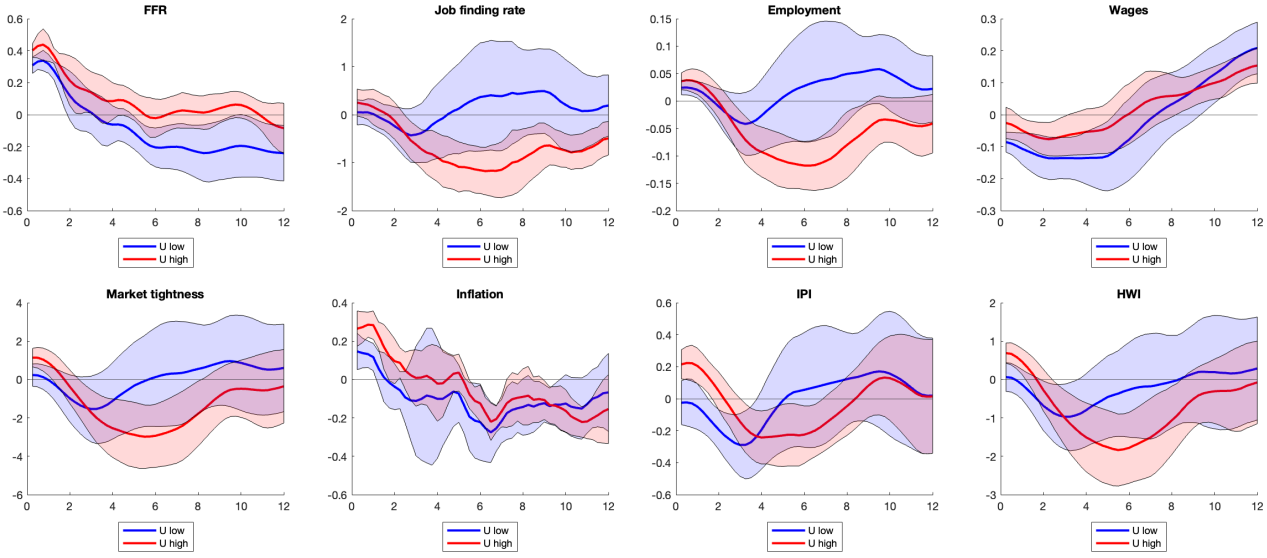

Notes: Six lags, 90% confidence intervals (asymptotic). Sample 1969-2007, monthly frequency. $\lambda_1 = 200, \lambda_2 = 20$, $\lambda_3 = 0.1$. For the purpose of this figure, the local projections are evaluated in the 30^{th} percentile (low unemployment) and the 70^{th} percentile of unemployment (high unemployment) over the sample period.

Figure A2: State-Dependent Impulse Response Functions using Gertler-Karadi shocks

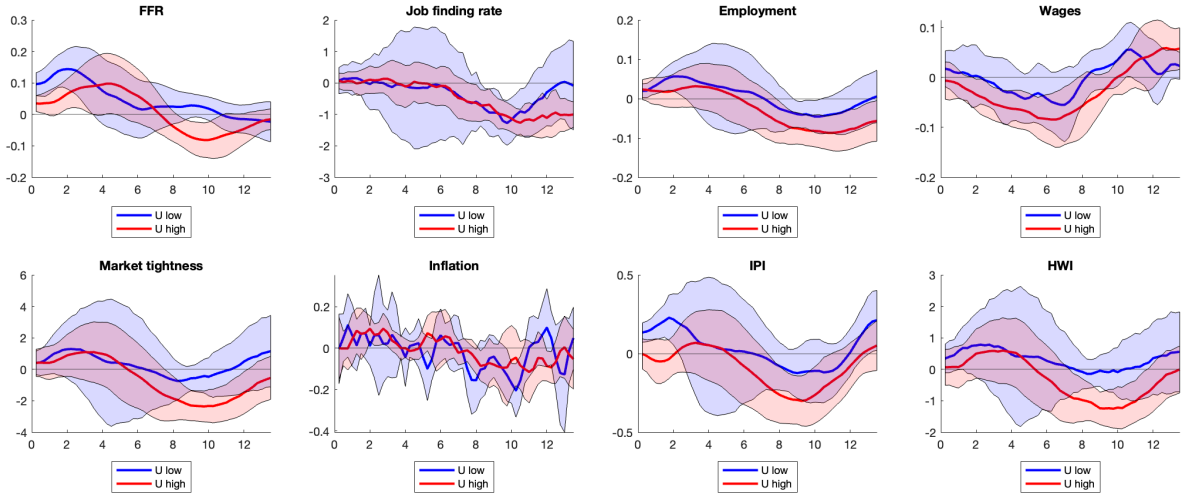

Notes: 90% confidence bands (asymptotic). Two lags. Shocks used are the residuals of the original shock series, regressed on 12 months of changes in FFR. Sample 1990-2012, monthly frequency. Shrinkage parameters: $\lambda_1 = 4, \lambda_2 = 0.05$, $\lambda_3 = 0$. The local projections are evaluated in the 30^{th} percentile (low unemployment) and the 70^{th} percentile of unemployment (high unemployment) over the sample period.

Figure A3: State-Dependent Impulse Response Functions using Romer-Romer shocks: unemployment and TFP

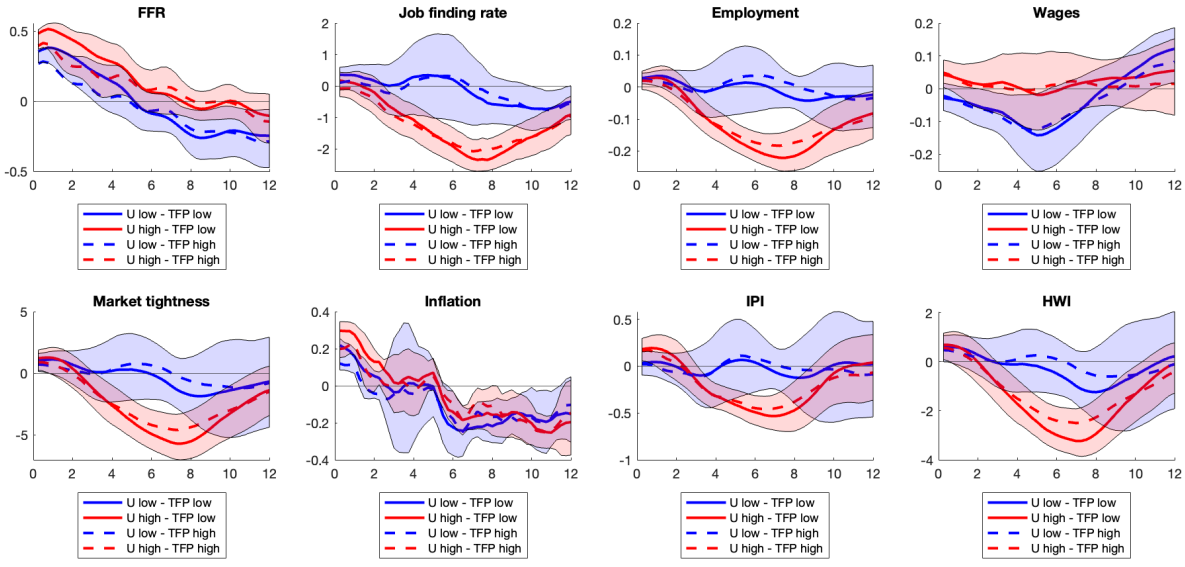

Notes: 4 lags, sample 1969-2007, monthly frequency. $\lambda_1 = 200, \lambda_2 = 20, \lambda_3 = 0.1$. Local projections are evaluated in the 30^{th} percentile (low unemployment and low TFP growth respectively) and the 70^{th} percentile of unemployment (high unemployment and high TFP growth respectively). Dashed lines are high TFP growth, solid lines are low TFP growth. Red is High Unemployment, Blue is Low Unemployment. 90% confidence intervals (asymptotic) correspond to the IRF of having high unemployment and low unemployment, respectively, with median TFP growth (not visualized).

Figure A4: Asymmetric Impulse Response Functions using Romer-Romer shocks, controlling for state-dependence in unemployment

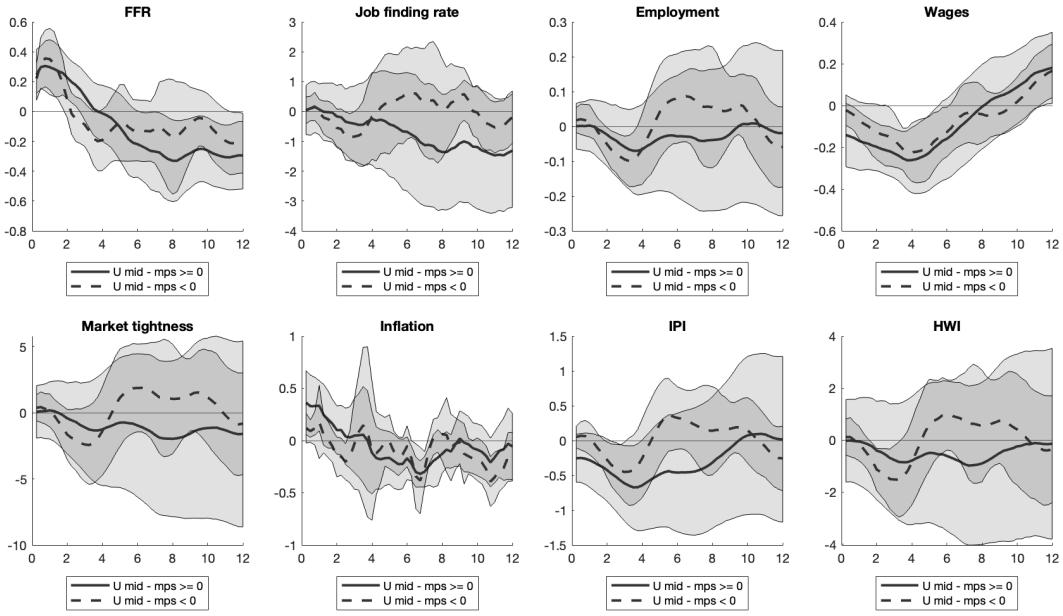

Notes: 4 lags, sample 1969-2007, monthly frequency. $\lambda_1 = 50, \lambda_2 = 1, \lambda_3 = 50, \lambda_4 = 10$. The local projections are evaluated in the 50th percentile of unemployment. 90% confidence intervals (asymptotic). Solid line is positive monetary policy shock, dashed line non-positive.

Figure A5: Asymmetric and State-dependent Impulse Response Functions using Romer-Romer shocks

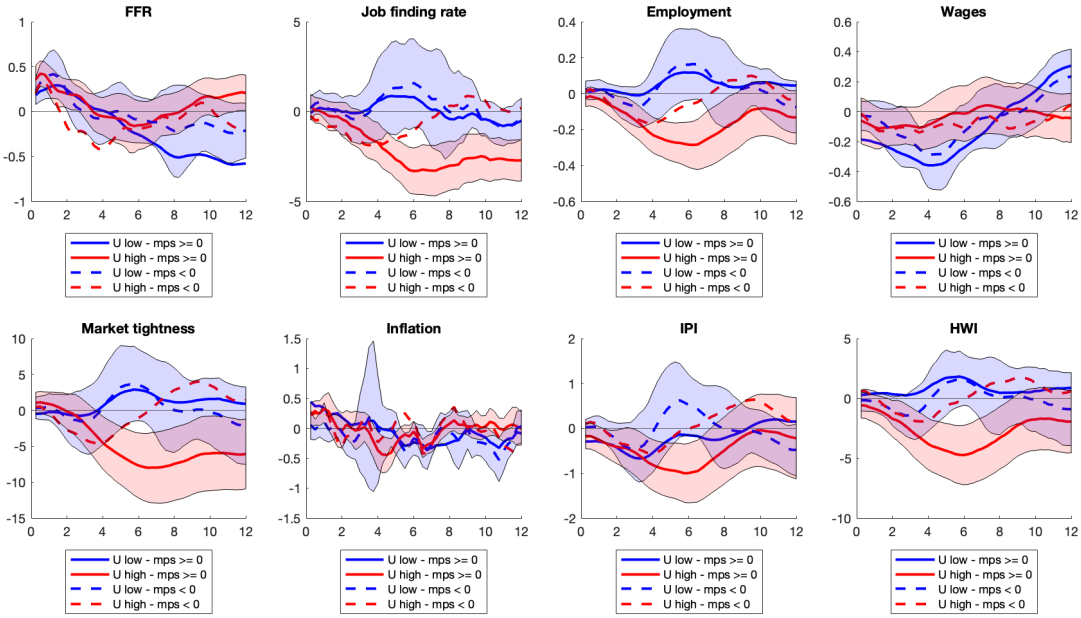

Notes: 4 lags, sample 1969-2007, monthly frequency. $\lambda_1 = 50, \lambda_2 = 1, \lambda_3 = 50, \lambda_4 = 10$. The local projections are evaluated in the 30th and 70th percentile of unemployment. 90% confidence intervals (asymptotic) visualized for the red solid line and the blue dashed line.

C Linear Model with Linear Estimates

Figure C1: Ergodic sets of linear model evaluated in linear parameter estimates of Table 1

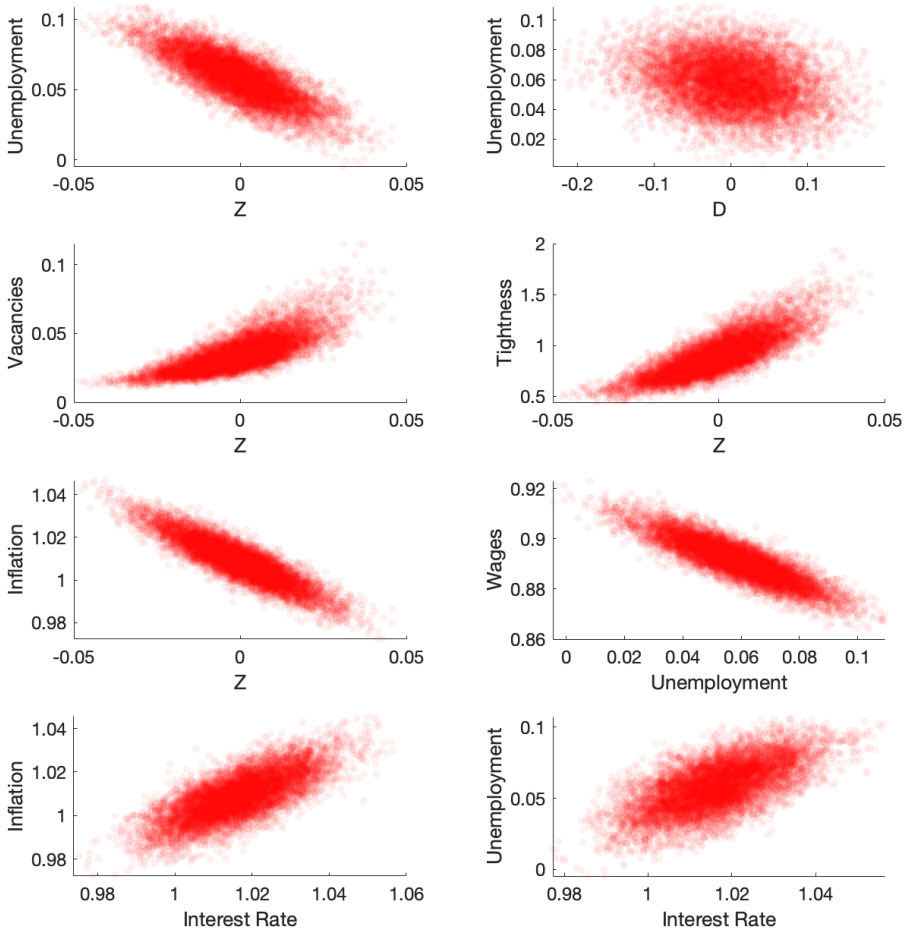

Figure C2: Impulse response functions of linear model evaluated in linear parameter estimates of Table 1

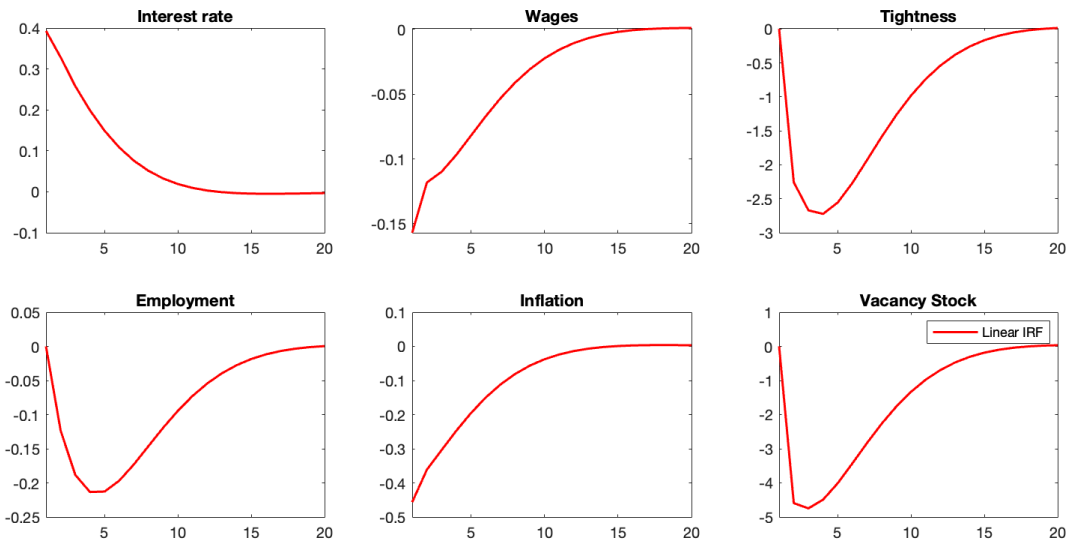

D Analytical log-linearization

D.1 Smaller version of the model

In the first part of this Appendix section, we consider a smaller version of the model, for which we analytically derive a set of log-linearized first-order conditions. Compared to the main model in the text, this model leaves out the following elements: (i) discount factor shocks, (ii) long-lived vacancies (i.e., we only consider a flow, not a stock), (iii) quadratic vacancy cost, and (iv) external habits in the utility function of the households.

D.1.1 Equilibrium Conditions

$$1 = \beta E_t \left[\frac{R_t}{\pi_{t+1}} \left(\frac{C_{t+1}}{C_t} \right)^{-\tau} \right] \tag{D.1}$$

$$\frac{\omega_t}{\gamma} - 1 = -\phi(\pi_t - \pi)\pi_t + \phi \mathbb{E}_t \left[Q_{t,t+1}(\pi_{t+1} - \pi)\pi_{t+1} \frac{Y_{t+1}}{Y_t} \right] \tag{D.2}$$

$$C_t = Y_t = Z_t N_t \tag{D.3}$$

$$N_t = (1-\delta)N_{t-1} + q_t V_t \tag{D.4}$$

$$\ln Z_{t+1} = \rho_z \ln Z_t + \epsilon_{z,t+1} \tag{D.5}$$

$$q_t = \chi \left(1 + \theta_t^{\iota}\right)^{\frac{-1}{\iota}} \tag{D.6}$$

$$\theta_t = \frac{V_t + X_t}{1 - (1-\delta)N_{t-1}} \tag{D.7}$$

$$\frac{\kappa}{q_t} = (1-\omega_t)Z_t - w_t + (1-\delta)E_t \left[Q_{t,t+1} \frac{\kappa}{q_{t+1}} \right] \tag{D.8}$$

$$w_t = \eta(1-\omega_t)Z_t + (1-\eta)\nu + \eta(1-\delta)\kappa E_t \left[Q_{t,t+1}\theta_{t+1} \right] \tag{D.9}$$

$$\frac{R_t}{\bar{R}} = \left[\left(\frac{\pi_t}{\bar{\pi}} \right)^{\psi_1} \left(\frac{Y_t}{\bar{Y}} \right)^{\psi_2} \right]^{1-\rho_R} \left(\frac{R_{t-1}}{\bar{R}} \right)^{\rho_R} e^{\epsilon_{R,t}} \tag{D.10}$$

D.1.2 Steady State

We consider a steady state with $\pi = 1$.

$$\pi = 1 \tag{D.11}$$

$$R = \beta^{-1} \tag{D.12}$$

$$\omega = \gamma \tag{D.13}$$

$$Z = 1 \tag{D.14}$$

$$C = Y = N \tag{D.15}$$

$$\delta N = qV \tag{D.16}$$

$$\theta = \frac{V}{1-(1-\delta)N} \tag{D.17}$$

$$q(\theta) = \chi\left(1+\theta^{\iota}\right)^{\frac{-1}{\iota}} \tag{D.18}$$

$$w = \eta\left[1-\gamma+(1-\delta)\beta\kappa\theta\right]+(1-\eta)\nu \tag{D.19}$$

$$w = 1-\gamma-\frac{\kappa}{q(\theta)}\left[1-(1-\delta)\beta\right] \tag{D.20}$$

D.1.3 Log-Linear Solution

$$E_t\left[\hat{y}_{t+1}\right] = \hat{y}_t + \frac{1}{\tau}E_t\left[\hat{r}_t - \hat{\pi}_{t+1}\right] \tag{D.21}$$

$$\hat{c}_t = \hat{y}_t = \hat{z}_t + \hat{n}_t \tag{D.22}$$

$$\hat{n}_t = (1-\delta)\hat{n}_{t-1} + \delta\left(\hat{q}_t + \hat{v}_t\right) \tag{D.23}$$

$$\hat{z}_t = \rho_z\hat{z}_{t-1} + \epsilon_{z,t} \tag{D.24}$$

$$\hat{r}_t = (1-\rho_R)\left[\psi_1\hat{\pi}_t + \psi_2\hat{y}_t\right] + \rho_R\hat{r}_{t-1} + \epsilon_{R,t} \tag{D.25}$$

$$\hat{\pi}_t = \beta E_t\left[\hat{\pi}_{t+1}\right] - \frac{1}{\phi}\hat{\omega}_t \tag{D.26}$$

$$\hat{w}_t = \frac{(1-\gamma)\hat{z}_t - \gamma\hat{\omega}_t + (1-\delta)\kappa\beta\theta E_t\left[\hat{\pi}_{t+1} - \hat{r}_t + \hat{\theta}_{t+1}\right]}{1-\gamma+\frac{1-\eta}{\eta}\nu + (1-\delta)\kappa\beta\theta} \tag{D.27}$$

$$\hat{q}_t = \frac{-1}{1+\theta^{\iota}}\hat{\theta}_t \tag{D.28}$$

$$\hat{\theta}_t = \hat{v}_t + \frac{(1-\delta)N}{1-(1-\delta)N}\hat{n}_{t-1} \tag{D.29}$$

$$\hat{q}_t = \frac{\gamma(1-\beta(1-\delta))}{1-\gamma-w}\hat{\omega}_t + \frac{(\gamma-1)(1-\beta(1-\delta))}{1-\gamma-w}\hat{z}_t + \frac{w(1-\beta(1-\delta))}{1-\gamma-w}\hat{w}_t + (1-\delta)\beta E_t[\hat{q}_{t+1} + \hat{r}_t - \hat{\pi}_{t+1}] \tag{D.30}$$

These ten equations determine the dynamics of the ten variables $\{\hat{y}_t, \hat{r}_t, \hat{\pi}_t, \hat{z}_t, \hat{n}_t, \hat{q}_t, \hat{v}_t, \hat{w}_t, \hat{\omega}_t, \hat{\theta}_t\}$.

D.2 Full Model

Next, analogously, we derive a set of log-linearized equations for the full model.

D.2.1 Equilibrium Conditions

$$\lambda_t = \beta D_t (C_t - bC_{t-1})^{-\tau} \tag{D.31}$$

$$1 = \beta E_t \left[\frac{R_t}{\pi_{t+1}} \frac{\lambda_{t+1}}{\lambda_t} \right] \tag{D.32}$$

$$\frac{\omega_t}{\gamma} - 1 = -\phi(\pi_t - \pi)\pi_t + \phi \mathbb{E}_t \left[Q_{t,t+1}(\pi_{t+1} - \pi)\pi_{t+1} \frac{Y_{t+1}}{Y_t} \right] \tag{D.33}$$

$$C_t = Y_t = Z_t N_t \tag{D.34}$$

$$N_t = (1-\delta)N_{t-1} + q_t (V_t + X_t) \tag{D.35}$$

$$V_{t+1} = (1-\xi)(1-q_t)(V_t + X_t) \tag{D.36}$$

$$\mu_t = (1-\omega_t)Z_t - w_t + (1-\delta)E_t [Q_{t,t+1}\mu_{t+1}] \tag{D.37}$$

$$X_t = \frac{q_t \mu_t - \kappa}{\psi_x} + (1-\xi)(1-q_t)E_t [Q_{t,t+1}X_{t+1}] \tag{D.38}$$

$$\mu_t = \frac{1-\eta}{\eta}(w_t - \nu) + (1-\delta)E_t [Q_{t,t+1}(1-\theta_{t+1}q_{t+1})\mu_{t+1}] \tag{D.39}$$

$$\frac{R_t}{\bar{R}} = \left[\left(\frac{\pi_t}{\bar{\pi}} \right)^{\psi_1} \left(\frac{Y_t}{\bar{Y}} \right)^{\psi_2} \right]^{1-\rho_R} \left(\frac{R_{t-1}}{\bar{R}} \right)^{\rho_R} e^{\sigma_R \epsilon_{R,t}} \tag{D.40}$$

$$q_t = \chi \left(1 + \theta_t^{\iota}\right)^{\frac{-1}{\iota}} \tag{D.41}$$

$$\theta_t = \frac{V_t + X_t}{1 - (1-\delta)N_{t-1}} \tag{D.42}$$

$$\ln Z_{t+1} = \rho_z \ln Z_t + \sigma_z \epsilon_{z,t+1} \tag{D.43}$$

$$\ln D_{t+1} = \rho_d \ln D_t + \sigma_d \epsilon_{d,t+1} \tag{D.44}$$

$$\tag{D.45}$$

D.2.2 Steady State

We consider a steady state with $\pi = 1$.

$$\pi = 1$$

$$\lambda = \beta\left((1-b)C\right)^{-\tau}$$

$$R = \beta^{-1}$$

$$\omega = \gamma$$

$$C = Y = N$$

$$\delta N = q(V+X)$$

$$V = (1-\xi)(1-q)(V+X)$$

$$\mu = \frac{1-\gamma-w}{1-(1-\delta)\beta}$$

$$X = \frac{q\mu-\kappa}{\psi_x} + (1-\xi)(1-q)\beta X$$

$$\mu = \frac{1-\eta}{\eta}(w-\nu) + (1-\delta)\beta(1-\theta q)\mu$$

$$q = \chi\left(1+\theta^{\iota}\right)^{\frac{-1}{\iota}}$$

$$\theta = \frac{V+X}{1-(1-\delta)N}$$

$$Z = 1$$

$$D = 1$$

D.2.3 Log-Linear Solution

$$
\begin{aligned}
\hat{\lambda}_t &= \hat{d}_t - \frac{\tau}{1-b}\left(\hat{y}_t - b\hat{y}_{t-1}\right) \\
\hat{\lambda}_t &= E_t\left[\hat{r}_t - \hat{\pi}_{t+1} + \hat{\lambda}_{t+1}\right] \\
\hat{y}_t &= \hat{z}_t + \hat{n}_t \\
\hat{n}_t &= (1-\delta)\hat{n}_{t-1} + \delta\hat{q}_t + \delta\left((1-\xi)(1-q)\hat{v}_t + \left[1-(1-\xi)(1-q)\right]\hat{x}_t\right) \\
\hat{v}_{t+1} &= \frac{q}{q-1}\hat{q}_t + (1-\xi)(1-q)\hat{v}_t + \left[1-(1-\xi)(1-q)\right]\hat{x}_t \\
\hat{\pi}_t &= \beta E_t\left[\hat{\pi}_{t+1}\right] - \frac{1}{\phi}\hat{\omega}_t \\
\hat{\mu}_t &= \frac{1-(1-\delta)\beta}{1-\gamma-w}\left[(1-\gamma)\hat{z}_t - \gamma\hat{\omega}_t - w\hat{w}_t\right] + (1-\delta)\beta E_t\left[\hat{\pi}_{t+1} - \hat{r}_t + \hat{\mu}_{t+1}\right] \\
\hat{x}_t &= \frac{q\mu\left[1-(1-\xi)(1-q)\beta\right]}{q\mu-\kappa}\left(\hat{q}_t + \hat{\mu}_t\right) - q(1-\xi)\beta\hat{q}_t + (1-\xi)(1-q)\beta E_t\left[\hat{\pi}_{t+1} - \hat{r}_t + \hat{x}_{t+1}\right] \\
\hat{\mu}_t &= \left[1-(1-\delta)\beta(1-\theta q)\right]\frac{w}{w-\nu}\hat{w}_t + (1-\delta)\beta(1-\theta q)E_t\left[\hat{\pi}_{t+1} - \hat{r}_t + \hat{\mu}_{t+1}\right] - (1-\delta)\beta\theta q E_t\left[\hat{\theta}_{t+1} + \hat{q}_{t+1}\right] \\
\hat{q}_t &= \frac{-1}{1+\theta^{\iota}}\hat{\theta}_t \\
\hat{\theta}_t &= (1-\xi)(1-q)\hat{v}_t + \left[1-(1-\xi)(1-q)\right]\hat{x}_t + \frac{(1-\delta)N}{1-(1-\delta)N}\hat{n}_{t-1} \\
\hat{r}_t &= (1-\rho_R)\left[\psi_1\hat{\pi}_t + \psi_2\hat{y}_t\right] + \rho_R\hat{r}_{t-1} + \epsilon_{R,t} \\
\hat{z}_t &= \rho_z\hat{z}_{t-1} + \epsilon_{z,t} \\
\hat{d}_t &= \rho_d\hat{d}_{t-1} + \epsilon_{d,t}
\end{aligned}
$$

This is fourteen equations in fourteen unknowns $\left\{\hat{\lambda}_t, \hat{d}_t, \hat{y}_t, \hat{r}_t, \hat{\pi}_t, \hat{z}_t, \hat{n}_t, \hat{q}_t, \hat{v}_t, \hat{x}_t, \hat{\omega}_t, \hat{\mu}_t, \hat{w}_t, \hat{\theta}_t\right\}$